UiT The Arctic University of Norway

Department of Medical Biology

High Palmitate Alters Glutathione Redox During Severe Oxidant Stress in the Heart

An Evaluation of Altered Glutathione Redox Environment on Cardiac Function and Mitochondrial Energetics

Ramin Sepehrara

MSc Thesis in Biomedicine

MBI-3911

May 2021

Acknowledgments

I would like to thank my supervisor, Neoma Tove Boardman, for all her support and guidance during this MSc project. I thank the senior laboratory engineer, Trine Lund, for all her help every time I had a question and helping a lot during performing experiments, notably with the O2K, optimizing primers and 'GeNorm' software. A special thanks to Roy Lysså for designing the protocol to prepare glutathione samples, and Ole-Martin Fuskevåg for performing LC-MS/MS experiments and the data analysis. I am also thankful to my co-supervisors, Ellen Aasum and Anne Hafstad.

Ramin Sepehrara

May 18th, 2021,

Tromsø, Norway.

Abstract

When the heart is under stress, e.g. ischemia-reperfusion (IR), it produces an enormous amount of reactive oxygen species (ROS). Glutathione, which is an endogenous antioxidant derived from the 'nicotinamide adenine dinucleotide hydrogen' (NADH) of the 'tricarboxylic acid' cycle, can fight against this oxidative stress to balance the redox environment, and convert the produced ROS to H_2O. In this study, we hypothesized that elevated levels of fatty acids, such as palmitate, can contribute to maintain the ratio of reduced (GSH) and oxidized (GSSG) glutathione during cardiac stress. Therefore, the aim was to evaluate the potential effects of high levels of palmitate in hearts exposed to stress induced by IR or diamide pro-oxidant on cardiac function and mitochondrial energetics. Cardiac function was assessed in isolated working hearts perfused with low and high concentrations of palmitate. Following that, mitochondrial respiration and hydrogen peroxide (H_2O_2) emission were determined using a high-resolution respirometry and fluorometry (Oxygraph-2k, OROBOROS Instruments, Innsbruck, Austria). Liquid chromatography tandem mass spectrometry was used to measure GSH and GSSG levels, and GSH/GSSG. Changes in the expression of various genes related to mitochondrial dynamics and GSH were evaluated using real time-reverse transcription polymerase chain reaction. Lastly, protein S-glutathionylation was determined using western blotting. We observed that although IR and diamide treatments could significantly alter the cardiac function, including the cardiac output, cardiac power, and aortic flow, only the diamide treatment altered the levels of GSH, GSSG, and GSH/GSSG. In addition, diamide treatment altered mitochondrial respiration and H_2O_2 emission. The presence of high palmitate during diamide treatment resulted in lower levels of GSSG as compared to hearts perfused with low palmitate. Also, mRNA expression of '*glutathione reductase*' (*grs*) and '*glutathione synthetase*' (*gss*), two genes related to GSH synthesis, were different in hearts perfused with low and high palmitate levels, respectively. However, in-depth studies should be performed to evaluate the role of palmitate in GSH synthesis and oxidation.

Abbreviations

ADP: adenosine diphosphate

ATP: adenosine triphosphate.

BSA: bovine serum albumin.

CCCP: carbonyl cyanide m-chlorophenylhydrazone.

cDNA: complementary deoxyribonucleic acid.

CI: complex I.

CII: complex II.

CIII: complex III.

CIV: complex IV.

CoA: coenzyme A.

CS: citrate synthase.

CV: complex V.

ddH_2O: double distilled water.

dNTP: deoxynucleoside triphosphate.

DTNB: dithionitrobenzoic acid.

EDTA: ethylenediaminetetraacetic acid.

ETS: electron transport system.

$FADH_2$: flavin adenine dinucleotide hydrogen.

GAPDH: glyceraldehyde 3-phosphate dehydrogenase.

GSH/GSSG: reduced glutathione per oxidized glutathione ratio.

GSH: reduced glutathione.

GSSG: oxidized glutathione.

H_2O: water.

H_2O_2: hydrogen peroxide.

HCl: hydrochloric acid.

HMBS: hydroxymethylbilane synthase.

HP: high palmitate.

HP+DMD: high palmitate+diamide.

HPRT: hypoxanthine guanine phosphoribosyl transferase.

HRP: horseradish peroxidase.

IMM: inner mitochondrial membrane.

IR: ischemia-reperfusion.

KHB: Krebs-Henseleit buffer.

LC-MS/MS: liquid chromatography tandem mass spectrometry.

LP: low palmitate.

LP+DMD: low palmitate+diamide.

MiR05: mitochondrial respiration medium 05.

MnSOD: superoxide dismutase.

mRNA: messenger ribonucleic acid.

NADH: nicotinamide adenine dinucleotide hydrogen.

NADPH: nicotinamide adenine dinucleotide phosphate hydrogen.

NEFA: non-esterified fatty acids.

NEM: n-ethylmaleimide.

O_2^-: superoxide anion.

OMM: outer mitochondrial membrane.

OXPHOS: oxidative phosphorylation.

ROS: reactive oxygen species.

RT: reverse transcriptase.

RT-PCR: real time-reverse transcription polymerase chain reaction.

SDHA: succinate dehydrogenase complex flavoprotein subunit A.

SDS: sodium dodecyl sulphate.

TBS-T: tris buffered saline-tween 20.

TCA cycle: tricarboxylic acid cycle.

TNB: thiobenzoic acid.

UV: ultraviolet.

β-ME: β-mercaptoethanol.

Table of Contents

List of Figures

List of Appendices Figures

List of Tables

List of Appendices Tables

1 Introduction

1.1 Background

In today's world cardiovascular diseases play a crucial role in death and disability [1]. Even though the mortality due to acute myocardial infarction has decreased in the last thirty years, heart failure leading to death has risen [1]. Although mostly the elderly, 6–10% of people who are over 65, are affected by heart failure, this disorder is present in between 1-2% of the population of adults [2]. The lifetime risk to develop heart failure for a 40-year old person is approximately one in five [2]. Although the incidence of heart failure which is linked to the age has not changed in the last twenty years, it is thought that the prevalence is increasing [2].

In the last century numerous cardiac abnormalities related to the structure and biochemistry of the heart have been associated with heart failure [1]. Among these, the ability of the myocardium to transfer the chemical energy from the carbon fuels metabolism to contractile work decreases and mitochondrial dysfunction may also occur [1].

1.2 Cardiac Metabolism

The energy demand of the heart is very high because it must continuously produce a high rate of ATP to maintain contractile function, basal metabolic processes, and ionic homeostasis [3]. Approximately thirty kilogram of ATP is produced and consumed by the heart each day yet it can store only small amounts enough for a few beats [4]. ATP is synthesized in mitochondria from various aerobic substrates, such as fatty acids (60–70%), carbohydrates (30%), and less frequently, amino acids and ketone bodies [4].

1.2.1 Fatty Acids β-Oxidation

Although ATP can be synthesized from many different substrates, the majority, 50–70%, of the ATP of the adult heart is obtained from the β-oxidation of fatty acids [3] (figure 1). β-oxidation of fatty acids contributes dynamically to the total oxidative energy metabolism of

the heart [3]. The range of this contribution can be from approximately 100% of the entire energy which is required by the heart to a minor involvement depending on the substrate availability, concentration, and the form of fatty acids which are transported to the heart, and whether the rival energy substrates are present [3]. β-oxidation of fatty acids is controlled at approximately all stages of the metabolic pathway, which includes lipoprotein lipase stage, the uptake of fatty acid to the cardiac myocyte, esterification to CoA, uptake by mitochondria, and β-oxidation [3]. The metabolic demand, TCA cycle and ETS activities can also regulate β-oxidation of fatty acids rate [3].

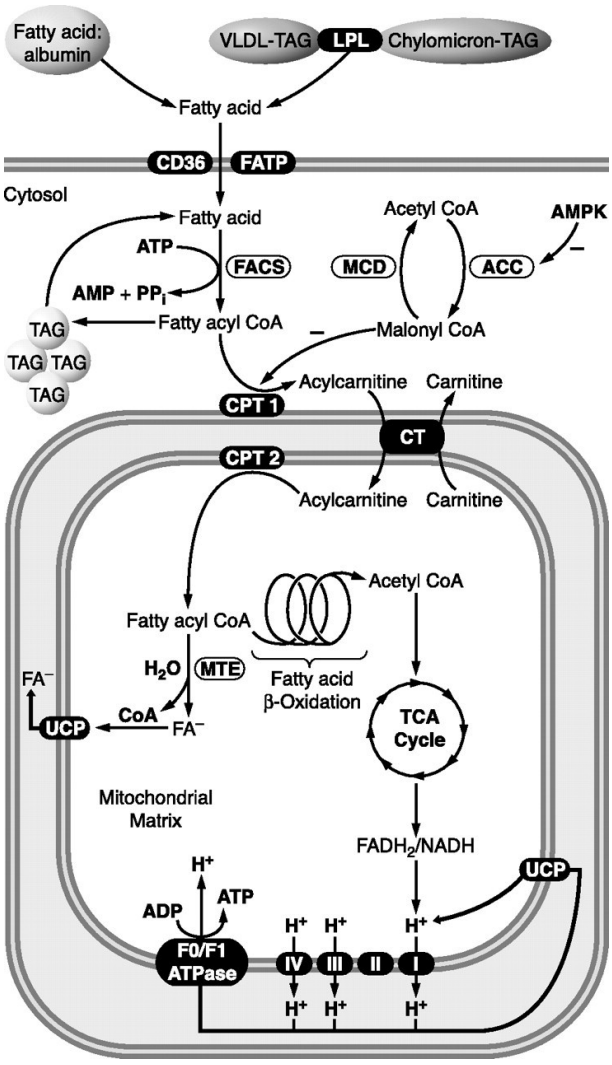

Figure 1. An overview of the heart's fatty acids β-oxidation. Fatty acyl coenzyme A (CoA) synthase (FACS) esterifies the fatty acids to fatty acyl CoA in the cytosol [3]. Transporting of the acylcarnitine to the mitochondria happens where carnitine palmitoyl transferase 2 (CPT 2) converts it back to fatty acyl CoA [3]. Most of this fatty acyl CoA enters the cycle of fatty acid β-oxidation to produce acetyl CoA, nicotinamide adenine dinucleotide hydrogen (NADH), and flavin adenine dinucleotide hydrogen ($FADH_2$) [3].

Under conditions such as fasting, and or in obesity or diabetes, high levels of circulating free fatty acids lead to increased use of fatty acids by the heart through increased fatty acids β-oxidation [5] (figure 2). In addition, acute myocardial infarction (heart attack) is associated with increased circulating levels of fatty acids due to a hyperadrenergic state and the increased rate of lipolysis in adipose tissue [6] [7]. The exposure to acutely elevated fatty acids levels may also cause further damage to the heart as fatty acids have also been associated with reduced cardiac efficiency, mitochondrial dysfunction, and oxidative stress [8] [9]. However, whether elevated fatty acids levels contribute to injury following myocardial IR is not completely clear [10].

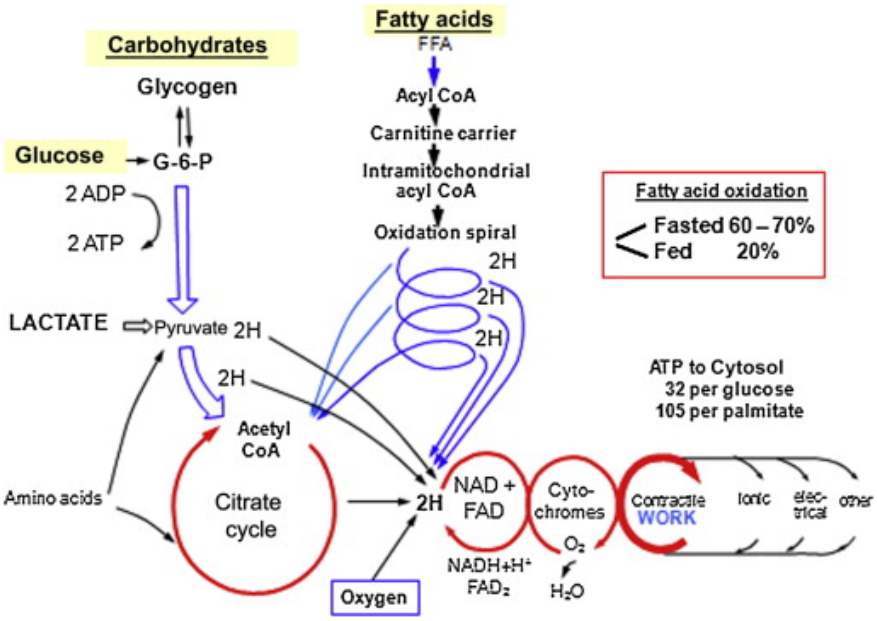

Figure 2. How energy is produced by carbohydrates and fatty acids for the heart to contract. Fuels, such as glucose and fatty acids, enter the tricarboxylic acid (TCA) cycle in mitochondria [5]. The contractile work utilizes the adenosine triphosphate (ATP) formed by the protons (H^+) produced by these fuels [5].

1.3 Mitochondrial Metabolism

1.3.1 Tricarboxylic acid (TCA) Cycle

There are complex metabolic pathways in the heart that transform the metabolic substrates, such as fatty acids, into acetyl CoA [3] (section 1.2.1). Glucose metabolism, where glucose is

oxidized to form pyruvate, can also form acetyl CoA [11] (figure 3). The chemical energy from acetyl CoA is transferred to the reducing power of NADH in the TCA cycle and is an important component of cell respiration and ATP production [12]. The rate of the TCA cycle is important in the control of ATP production by the heart [13].

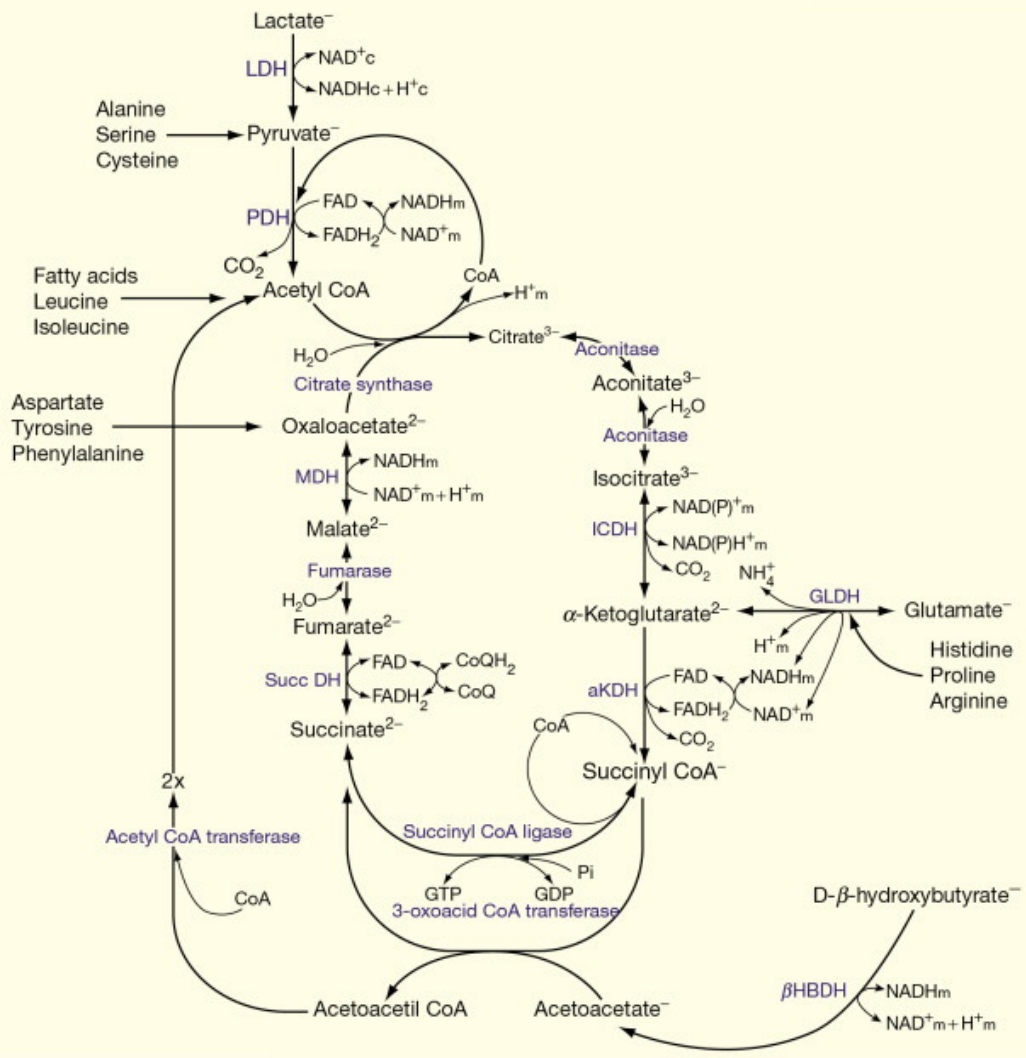

Figure 3. The fundamental pathway to degrade major foodstuffs, including carbohydrates, lipids, and proteins completely is tricarboxylic acid (TCA) cycle. This pathway also produces reducing equivalents transferred to the mitochondrial electron transport system (ETS) [11]. Adenosine triphosphate (ATP) synthesis is powered by the mitochondrial proton (H^+) gradient which is generated by these reducing powers redox reactions energy [11].

Fatty acids β-oxidation and the entry of acetyl CoA increases NADPH regeneration in the TCA cycle, and NADPH is used by 'glutathione reductase' (GRS) to convert back GSSG to GSH [12]

[14] [15]. As GSH is a major cellular antioxidant and has a central role in redox homeostasis [14], fatty acids can therefore contribute to the maintenance of redox balance in the cells [15].

1.3.2 Electron Transport System (ETS)

This system consists of five complexes, CI, CII, CIII, CIV, and CV, better known as the ATP-synthetase or F0-F1-ATPase [16]. The NADH and $FADH_2$ which are produced in glycolysis, fatty acids oxidation, and TCA cycle are used to generate ATP by the ETS [16]. The current of electrons start when NADH binds to CI, or $FADH_2$ or succinate binds to CII and ATP synthesize is done in CV [16]. The electrons are transferred from the reducing equivalents of CI and CII to CIII through coenzyme Q [16]. Further, cytochrome C carries electrons from CIII to CIV [16]. ATP is regenerated when protons pass the IMM through ATP synthase and ADP is phosphorylated [16] (figure 4).

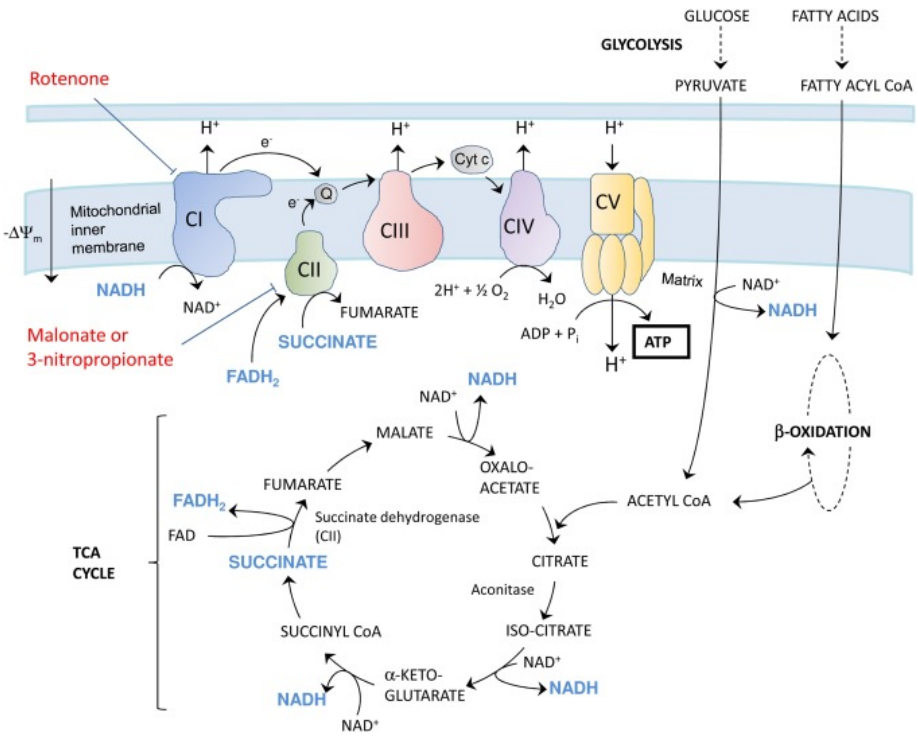

Figure 4. An overview of electron transport system (ETS) and tricarboxylic acid (TCA) cycle in mitochondria. Electrons are passed down through the respiratory complexes in the ETS [16]. Protons (H^+) pass through the inner mitochondrial membrane (IMM) via the CV (complex V) of the ETS where adenosine diphosphate (ADP) is phosphorylated to adenosine triphosphate (ATP) [16]. Nicotinamide adenine dinucleotide hydrogen (NADH), flavin adenine dinucleotide hydrogen ($FADH_2$), and succinate are produced in the TCA cycle [16].

1.3.2.1 Oxidative Phosphorylation (OXPHOS)

In OXPHOS, ATP synthesis is coupled to the ETS via an electrochemical transmembrane gradient [17]. The gradient is formed by the pumping of protons out across the inner mitochondrial membrane, also called the protons motive force, and it drives the phosphorylation of ADP because protons reenter the mitochondrial matrix through the ATP synthetase [18]. This complex acts like a molecular motor and ATP is formed by the proton movements that are caused by the transmembrane gradient [18].

1.3.2.2 Coupled versus Uncoupled Respiration

Overall, in coupled respiration there is a direct link between the rate of mitochondrial respiration and ATP synthesis by phosphorylating ADP which is regulated by a feedback mechanism corresponding to the demand of the cell for ATP [19]. In this mechanism, the F0-F1-ATP synthase uses the electrochemical proton gradient in the mitochondria generated while electrons are being passed down in the ETS, and this drives the ATP synthesis [20]. The respiratory complexes in the ETS have a crucial role in pumping protons out of the IMM to make a proton gradient which allows the ATP synthesis reactions to continue [19].

In noncoupled respiration, while the protons are still being used, the ATP synthesis decreases [21] [20]. This mechanism consumes the proton gradient of mitochondria and is called mitochondrial proton leak which is not coupled to ATP synthesis [21] [20] (figure 5). Therefore, there is no energy production and instead there is a passive leak of protons back into the mitochondrial matrix [21] [20].

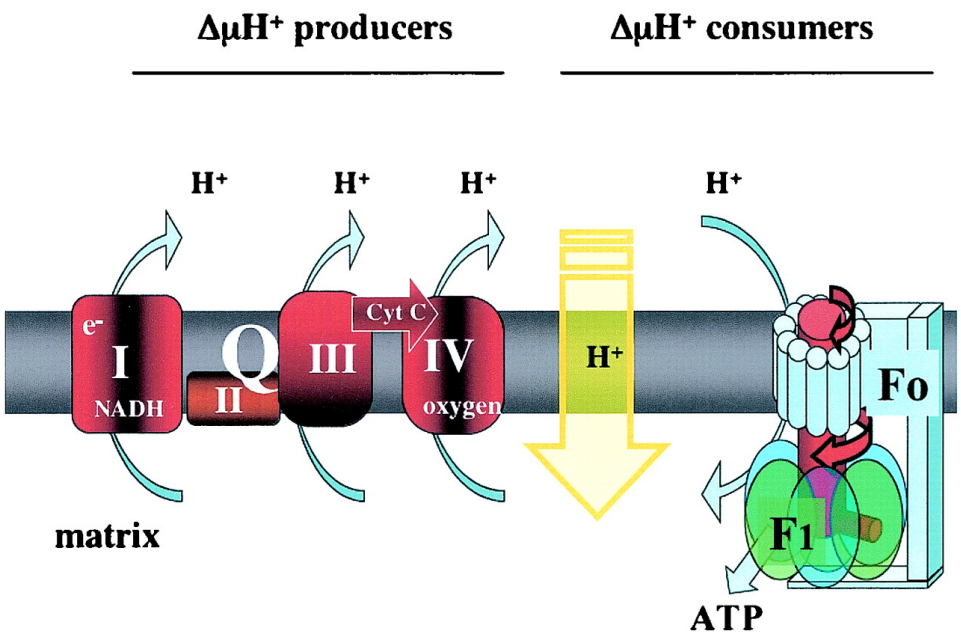

Figure 5. Coupled versus noncoupled mitochondrial respiration. In coupled respiration, to phosphorylate adenosine diphosphate (ADP), F0-F1-ATP synthase utilizes the proton (H^+) gradient that the mitochondrial respiratory chain complexes generate [20]. In the respiration mechanism noncoupled with ATP synthesis, which is called mitochondrial proton leak (yellow arrow), there is no energy production when protons (H^+) reenter the mitochondrial matrix [20].

1.3.2.3 Mitochondrial Reactive Oxygen Species (ROS) Production

When oxygen is not reduced completely, ROS are produced which contain either radical or non-radical oxygen species [22] (figure 6). Some types of ROS are O_2^-, H_2O_2, and hydroxyl radical ($HO^\bullet$) [22]. Mitochondrial OXPHOS can generate endogenous ROS in the cells [22]. CI and CIII are main sites of mitochondrial ROS production [23]. Oxidative stress happens when the system of antioxidant defense in the cells is outweighed by ROS, when there is a rise in the levels of ROS, or when the capacity of the antioxidant defense system of the cells declines [22].

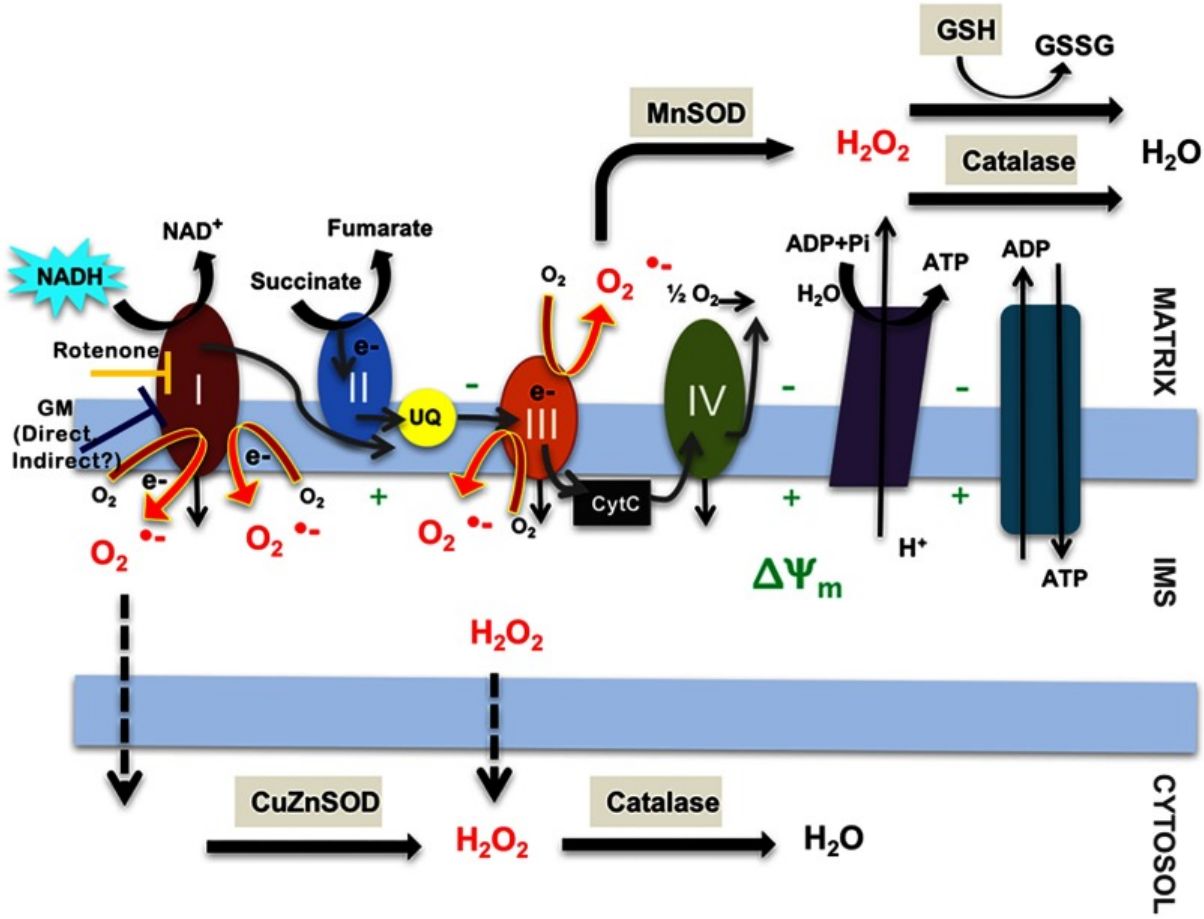

Figure 6. The production of reactive oxygen species (ROS) in electron transport system (ETS). Small amounts of ROS, mostly in the type of superoxide anion (O_2^-), are yielded by mitochondria when they are metabolizing normally [24]. MnSOD quickly converts O_2^- to hydrogen peroxide (H_2O_2) once it is released in the mitochondrial matrix [24]. CuZnSOD also does the conversion of O_2^- to H_2O_2 if there is a leakage of O_2^- to the intermembrane space resulting in leaking to the cytosol [24]. In the cytoplasm, however, glutathione (GSH) and catalase break down H_2O_2 to H_2O [24].

During reperfusion after acute myocardial ischemia the heart goes under a huge burst of ROS produced by the mitochondria [25] (figure 7). During ischemia the heart experiences hypoxia and uses anerobic respiration [25]. In line with this, the protons are pumped out of cardiomyocytes and the pH in the cardiomyocytes decreases [25]. Mitochondrial permeability transition pores (MPTPs) are also closed and the myofibrils contractility is inhibited [25]. On the contrary, when the blood flows back to the heart during reperfusion the accumulated lactic acid is washed out of the cardiomyocytes, the physiological pH is restored, and OXPHOS is resumed which causes a release of ROS [25]. During early reperfusion when the

concentration of Ca^{2+} may be high and the pH is not yet physiological, the myofibrils are hypercontracted [25]. This can also contribute to opening of the MPTPs and injure mitochondria [25].

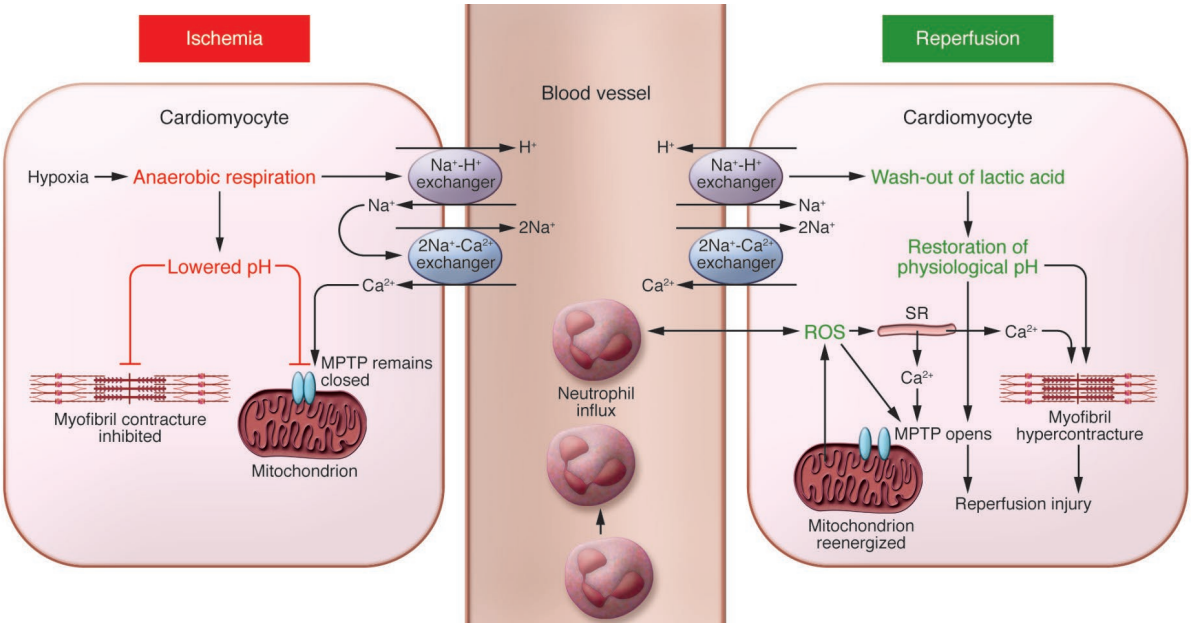

Figure 7. Following acute myocardial ischemia, the heart experiences an enormous production of reactive oxygen species (ROS) during the period of reperfusion. During ischemia the heart is in a hypoxic condition and utilizes anaerobic respiration [25]. In this period, the pH lowers and myofibrils do not contract [25]. In contrast, during reperfusion period, the lactic acid is washed out, pH returns to the physiological conditions and myofibrils are hypercontracted [25]. In addition, a burst of ROS production from mitochondria occurs during reperfusion [25].

1.4 Redox Environment and the Glutathione (GSH) Antioxidant System

The intracellular redox environment is considered to be the collection of an estimated 80,000 cysteines within the proteome that undergo reversible redox reactions [26]. Thiol antioxidant redox couples, such as GSH/GSSG, can influence the redox environment [27] by eradicating mitochondrial ROS accumulation [28]. On the other hand, GSH can bind to cysteine thiols and form disulfide bridges [27].

Because GSH can do the reduction of sulfur to hydrogen sulfide, it was formerly called ‘philothion’, which are two Greek words for love and sulfur, by Joseph de Rey-Pailhade [29]. Later, its physiological significance was discovered by Frederick G. Hopkins in 1921 and the

chemical structure was narrowed down to glutamate and cysteine which led to a name change to “glutathione” [29] (figure 8). GSH is generated from GSSG by glutathione reductase (GRS), which is an NADPH-dependent flavoenzyme [29]. The NADPH which is a prerequisite for glutathione synthesis originates from the TCA cycle [30]. To control the activity of proteins and defend against permanent overoxidation, GSH can form mixed disulfide bonds with them [29]. Glutaredoxin (GRX) catalyzes the deglutathionylation of disulfides which are mixed with GSH [29]. Glutathione peroxidase (GPX) oxidizes GSH to glutathione disulfide (GSSG) [31].

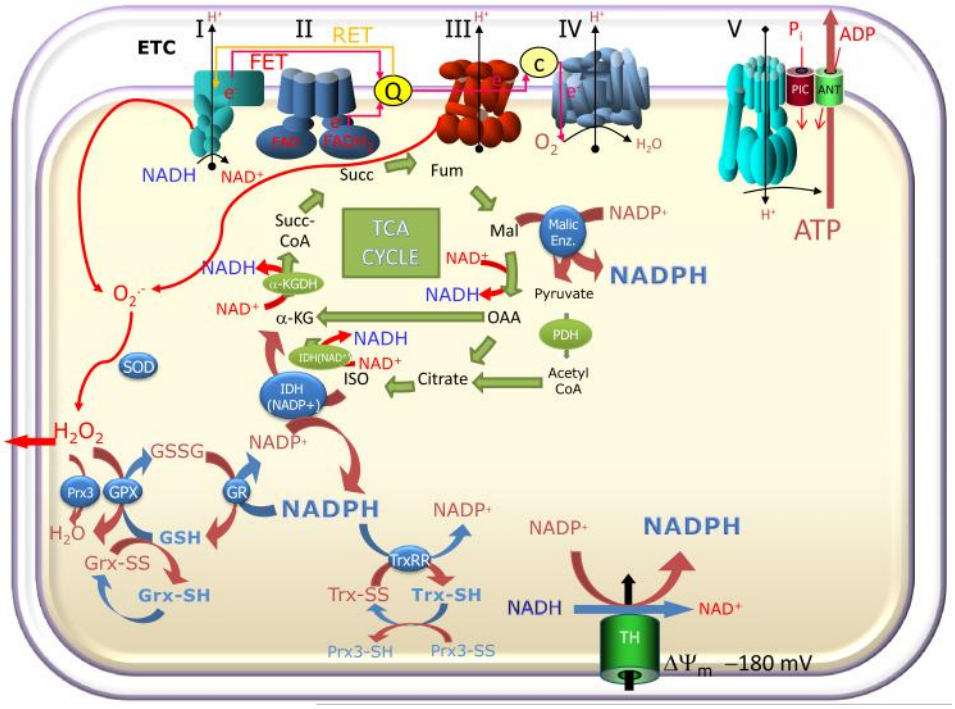

Figure 8. Mitochondrial antioxidant pathways. The tricarboxylic acid (TCA) cycle nicotinamide adenine dinucleotide phosphate hydrogen (NADPH) is necessary for glutathione synthesis [30]. Glutathione reductase (GRS), which is dependent on NADPH, converts back glutathione disulfide (GSSG) to its reduced form (GSH) [30]. The deglutathionylation of disulfides which are mixed with GSH is catalyzed by glutaredoxin (GRX) [30]. GSH is oxidized to GSSG by glutathione peroxidase (GPX) [30].

1.4.1 Protein S-glutathionylation

Protein S-glutathionylation, which is an oxidative modification of proteins, is a procedure in which mixed disulfides are formed between GSH and protein cysteines in oxidizing situations [29] (figure 9). In non-stressed cells, S-glutathionylation occurs only in less than 0.1% of total

protein cysteines while in different conditions of oxidative stress this number can increase to up to 15% [29].

When there is oxidative stress, redox modulation targets the residues of cysteine which are present on proteins with a low pKa [32]. Sulfenic, sulfinic, and sulfonic acids are formed by oxidation of cysteine residue in proteins [32]. The reduction or conjugation of sulfenic and sulfinic acids of proteins to GSH leads to S-glutathionylation of proteins and can occur through glutathione S-transferases (GST), glutaredoxin (GRX), or without using enzymes [32]. Glutaredoxin can reverse the post-translational glutathionylation modification [32].

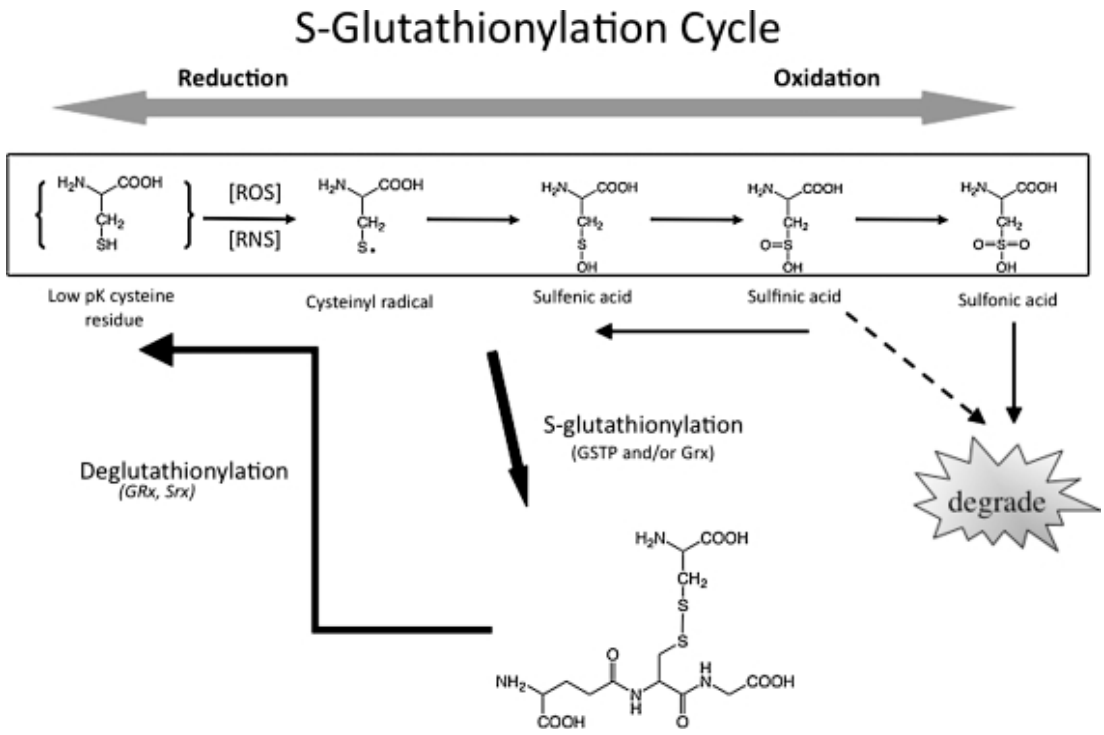

Figure 9. The cycle of S-glutathionylation. Protein S-glutathionylation occurs through glutathione S-transferases (GST), glutaredoxin (GRX), or without using any enzymes when sulfenic and sulfinic acids of proteins conjugate with glutathione (GSH) in oxidative stress [32]. The post-translational glutathionylation modification can be reversed by glutaredoxin (GRX) [32].

1.5 Mitochondrial Dynamic Proteins

Mitochondria are dynamically adapting to altered cellular and physiological conditions through fusion and fission [33]. Whereas fusion results in unified mitochondria, fission results in the fragmentation of mitochondria into smaller pieces [33]. Cells which are metabolically

active benefit from the large networks of mitochondria that fusion generates [33]. These networks have an important role in energy expenditure [33].

Mitochondrial fusion and fission mechanisms are balanced by mitochondrial shaping proteins [34]. Various proteins have been recognized to regulate these mechanisms [34]. OMMs are fastened by 'mitofusins' (MFN1 and MFN2) [34]. Remodeling of the cristae of mitochondria is sustained by 'optical atrophy 1' (OPA1) [34]. The IMMs' fusion is also driven by this gene [34]. Fission of mitochondrion, however, is modulated by 'dynamin-related protein 1' (DRP1) [34].

Two mitochondria are combined by mitochondrial fusion but in mitochondrial fission one mitochondrion is split into two mitochondria [35] (figure 10). 'Mitofusins' (MFN1 and MFN2) coordinate fusion on the OMM while 'optic atrophy 1' (OPA1) does the coordination of fusion on the IMM [35]. When the recruitment of endoplasmic reticulum (ER) to the site of constriction, which is marked by mtDNA, occurs fission starts [35]. Then, this type of constriction, which is facilitated by ER, is supported by 'dynamin-related protein 1' (drp1), which is recruited to mitochondrial surface by various proteins bound to OMM [35].

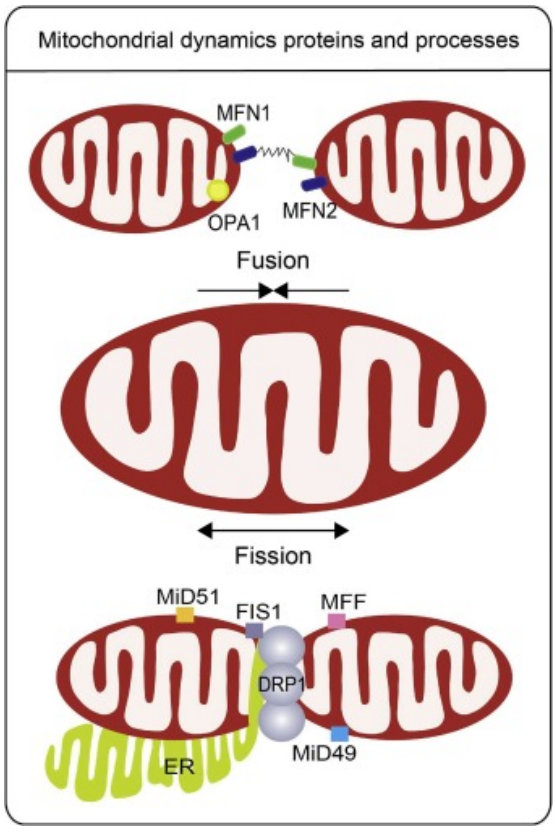

Figure 10. A simple overview of the fusion and fission mechanism of the mitochondria of human cells. Mitochondrial fusion occurs by 'mitofusins' (MFN1 and MFN2) on the outer mitochondrial membrane (OMM) and 'optic atrophy 1' on the inner mitochondrial membrane (IMM) [35]. 'Dynamin-related protein 1' (DRP1) is involved in mitochondrial fission [35].

2 Hypothesis and Aim

The GSH system can regulate mitochondrial energetics as well as cardiac function through the reversible S-glutathionylation of proteins in the heart, and is important during acute cardiac stress, such as IR. As fatty acids are known to contribute to replenish GSH, we hypothesized that heart perfusion with HP could contribute to maintaining GSH antioxidant system and balance GSH/GSSG redox environment during cardiac stress. The aim of this MSc project was to evaluate the effects of high levels of palmitate in isolated perfused murine hearts during altered GSH/GSSG redox environment such as under ischemic conditions or when using the chemical pro-oxidant diamide. We also aimed to see whether this was associated with changes in the cardiac and mitochondrial function, H_2O_2 emission, and expression of various genes related to mitochondrial dynamics and GSH antioxidant system. Finally, a global protein S-glutathionylation was performed to assess the general glutathionylated proteins under these conditions.

Overall, we have assessed in the present thesis whether or not elevated levels of palmitate, IR, and diamide pro-oxidant, could influence the cardiac function, GSH antioxidant system, mitochondrial energetics, H_2O_2 emission, and gene expression related to mitochondrial dynamics and GSH antioxidant, and evaluating glutathionylated proteins under HP levels, IR and diamide exposure.

3 Experiments and Analyses

3.1 Animals

Male C57Bl/6J mice, 10-12 weeks old were purchased from Charles River laboratory, Germany, and Janvier, France. Mice were housed with a 12:12 h light-dark cycle, and under constant conditions of temperature and humidity. They were given ad libitum access to food and water and treated in accordance with the guidelines on accommodation and care of animals (EU). All experiments were approved by the Animal Welfare Committee of the Arctic University of Norway (UiT).

Mice were administered an intra-peritoneal injection (IP) of heparin (100 units) prior to a lethal overdose of pentobarbital (100mg/ml). Hearts were excised and placed in ice-cold KHB (appendix I) (maximum of 2 minutes) before cannulation of the aorta in the perfusion system (section 3.2).

3.2 Isolated Working Heart Perfusion

All hearts were perfused in "working mode" under constant preload (10 mmHg) and afterload (50 mmHg), and the temperature of the heart was maintained at 37°C throughout the experiments. Hearts were perfused with modified KHB containing palmitate. Buffer is supplemented with glucose ($(C_6H_{12}O_6)$ (M=180.16 g/mol) [0.9 g/L]), and BSA ([30 g/L], pH 7.4) bound to palmitate. Further in the experiments these hearts were perfused with two different concentrations of palmitate, LP [0.35 mM] or HP [1.2 mM]. BSA was used as a binding protein to transport palmitate [36]. The buffer was oxygenated ($95\%O_2+5\%CO_2$) prior to the heart perfusion and during the perfusion. During heart excision, the aorta was cut proximal to the innominate artery base which provided 5-7 mm of aortic remnant for clamping and succeeding ligation of the aorta onto the canula [37].

The isolated hearts were exposed to three different treatments and perfused with either LP or HP, for a total of six groups (figure 11). For one treatment, they were perfused with either LP or HP buffer concentrations and underwent aerobic perfusion for approximately 35 minutes. For another treatment, hearts were perfused with LP or HP buffer and after a period of approximately 10-15 minutes for stabilization, buffer flow was stopped, and the heart underwent a global ischemia for 17 minutes followed by 5 minutes reperfusion. Finally, in another treatment, hearts were perfused with LP or HP buffer and 200 µM diamide ($(C_6H_{12}N_4O_2)$) which oxidizes thiols to disulfides [38]. As diamide is known to acutely regulate glutathione levels by oxidizing GSH to GSSG, this was also used as a positive control for GSH/GSSG analysis.

Following perfusion and prior to obtaining the heart weight, the heart was trimmed of fatty and other tissue and any excess fluid was removed. Samples of the heart were cut and

designated for either mitochondrial respiration, GSH analysis, or freezing in liquid nitrogen (N_2) for later analysis.

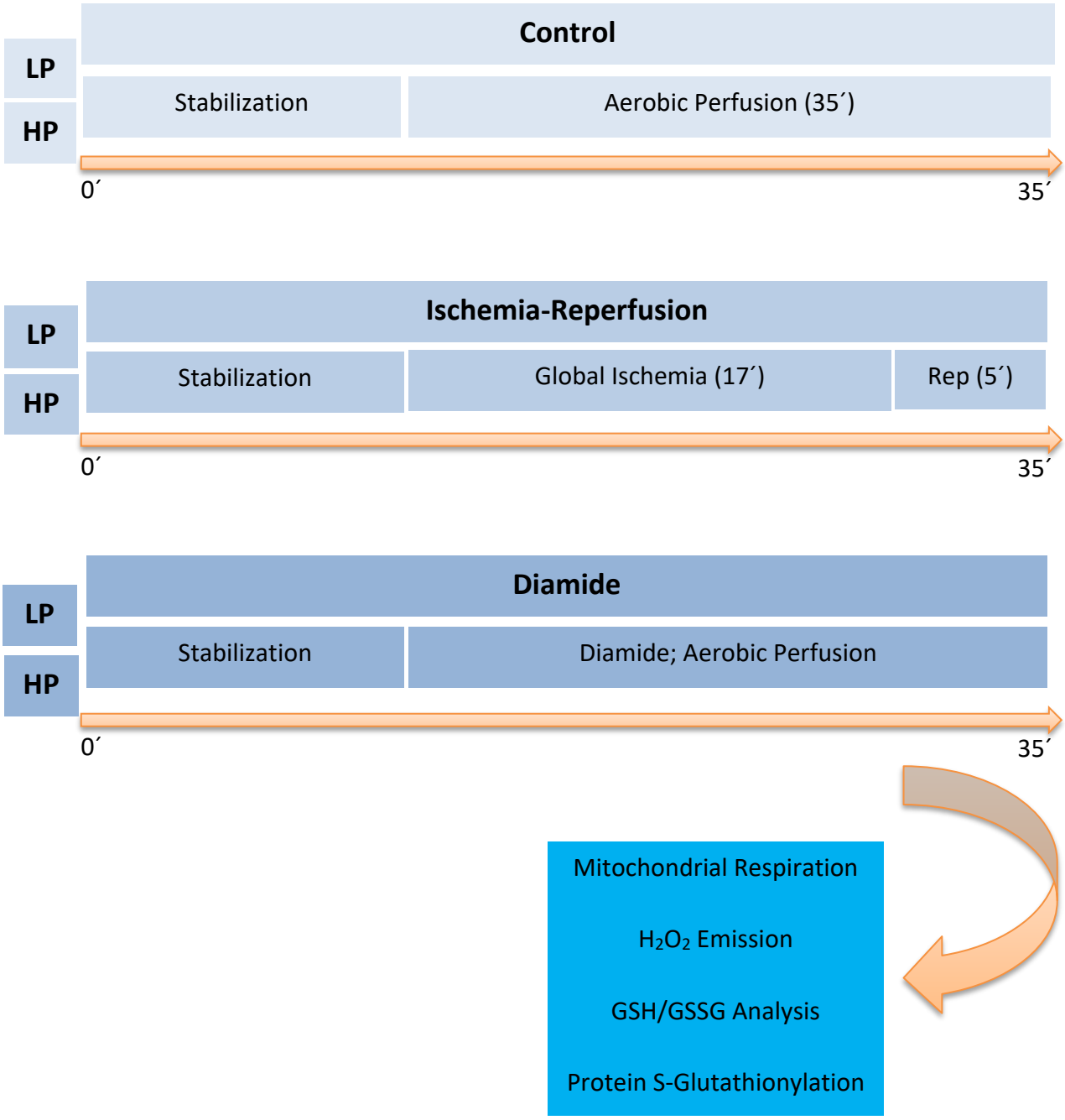

Figure 11. Experimental design. Hearts were perfused with either low palmitate (LP) or high palmitate (HP) buffer and were exposed to one of three different treatments: baseline conditions/aerobic perfusion, ischemia-reperfusion (IR), or diamide treatment. Rep: reperfusion. LP: low palmitate. HP: high palmitate. H_2O_2: hydrogen peroxide. GSH: reduced glutathione. GSSG: glutathione disulfide.

3.3 High-Resolution Respirometry (HRR) and Fluorometry (Hydrogen Peroxide (H_2O_2) Emission)

To measure mitochondrial respiration a high resolution respirometry (HRR) Oroboros O2k-FluoRespirometer instrument (Oxygraph-2k, OROBOROS Instruments, Innsbruck, Austria) was used (figure 12). The oxygen sensor of this instrument measures changes in the O_2 concentration over time and in parallel the O_2 flux (oxygen consumption rate), which is the derivative of the O_2 concentration, is calculated. ROS production was estimated by the levels of H_2O_2 emission. Mitochondrial H_2O_2 emission was measured simultaneously with respiration using Amplex® UltraRed, which is a fluorescent probe, and an O2k-Fluoroscence LED2-Module Fluorescence-Sensor Green, which produced fluorescence light. These will be described in detail in the sections below.

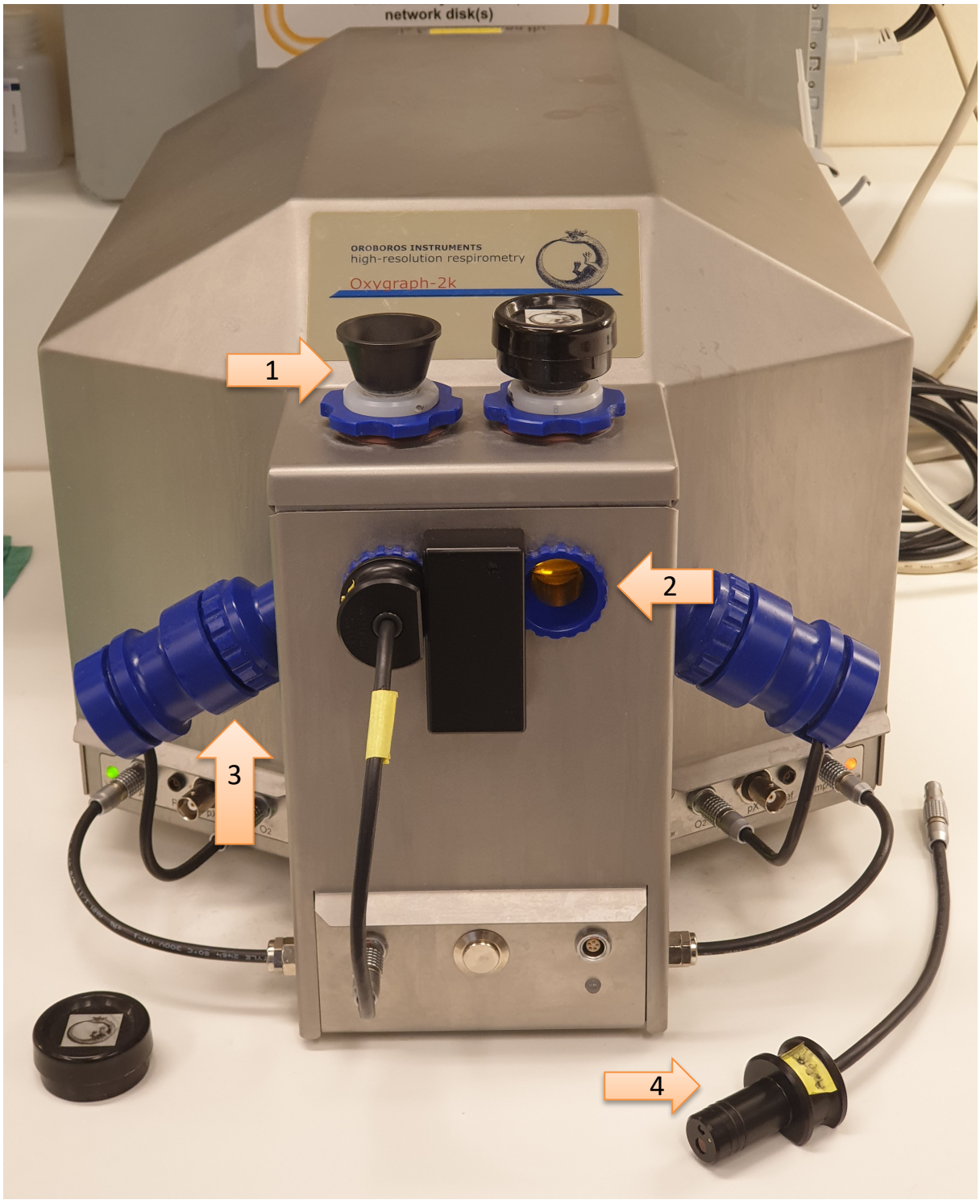

Figure 12. The Oroboros O2k-FluoRespirometer instrument allows the measurement of high resolution respirometry (HRR) and hydrogen peroxide (H_2O_2) emission at the same time. 1) The black PEEK stoppers with a central capillary which has 1.3 mm diameter and 50.6 mm length and are inserted into the chambers. 2) O2k-Window Frame where the O2k-Fluoroscence LED2-Module Fluorescence-Sensor Green is installed. 3) The OroboPOS polarographic oxygen sensor (POS). 4) O2k-Fluoroscence LED2-Module Fluorescence-Sensor Green.

3.3.1 Preparation of Tissue Samples

Following heart perfusions with the different treatments (figure 11), the heart was taken off the aorta cannula and place in ice-cold KHB. The heart was weighed and cut into four different pieces; for preparation of mitochondrial respiration, for mRNA analysis (see section 3.5), for analysis of GSH levels (see section 3.6), for analysis of overall protein S-glutathionylation (see section 3.8). The piece for mitochondrial respiration was taken from the ventricle and weighed before being placed in A1 solution (appendix II) which was used to keep the tissue biopsy under optimal conditions while cutting and for washing away the protease trypsin.

For this thesis, mitochondrial respiration and H_2O_2 emission were measured in cardiac homogenate. To prepare the cardiac tissue homogenate for mitochondrial respiration, the tissue was cut into small pieces, approximately 1 mm^3, in A1 solution with the protease trypsin. After ten minutes incubation with trypsin the tissue was washed with A1 solution and transferred to the lysis disc of the tube of a PBI-Shredder SG3 (OROBOROS Instruments, Innsbruck, Austria) (figure 13). MiR05 (appendix III) was added to the cap side of the tube and the tissue was homogenized for about twelve seconds using the shredder. Finally, the tissue homogenate was transferred to an Eppendorf tube. The entire procedure was done on ice except for the shredding step in which the lysis disc of the shredder tube was put on an ice-cold shredding stand.

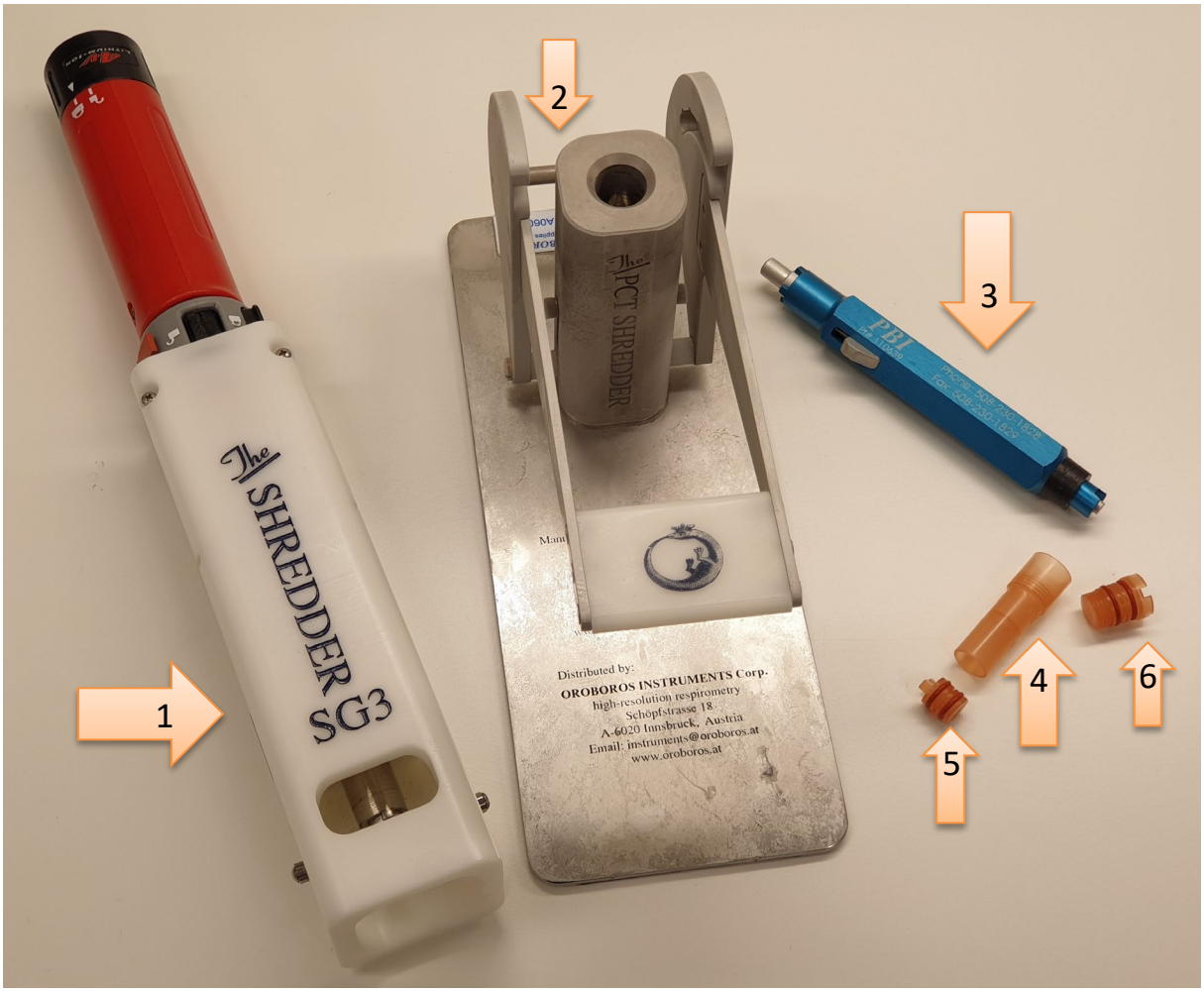

Figure 13. The PBI-Shredder SG3 which was used to homogenize the cardiac tissue. 1) Heavy duty high torque SG3 driver with convertible handle. 2) SG3 base with 3 position force setting lever (FSL). 3) Shredder-Tube Cap Tool. 4) Shredder Tube FT500-PS with Lysis Disk. 5) The rotating serrated Ram of the shredder tube. 6) The shredder tube cap.

3.3.2 Mitochondrial Respiration

Prior to performing each experiment, the O2k instrument was washed twice with ddH_2O and twice with MiR05. MiR05 is a physiological medium for mitochondrial respiration and is important for storing the tissue and performing mitochondrial respiration experiments by providing the necessary nutrients and desired pH (7.1). The MiR05 was kept in the chamber and the stoppers were opened to let an air bubble for a 20-minute incubation in the chamber to oxygenate the buffer. After that, the O2k was calibrated by selecting a section on the graph

and using it as the O_2 concentration. Then, the stoppers were closed, and excess buffer was removed such that the volume in the chamber was exactly 2 ml.

Various respiratory conditions such as LEAK and OXPHOS were of interest to be observed in these experiments in the O2k [39]. The LEAK state was determined when malate [0.4 M], pyruvate [2 M], and glutamate [2 M] were used as substrates (CI LEAK). This state represents the proton leak in CI prior to adding ADP and starting OXPHOS states. In contrast, OXPHOS was obtained when ADP [0.5 M] (CI OXPHOS) or succinate [1 M] (CI+CII OXPHOS) was added. The mitochondrial maximum capacity to respire was assessed using CCCP [1 mM] as a mitochondrial uncoupler. Cytochrome C [4 mM] was used as a test of mitochondrial membrane damage. Rotenone [1 mM] was used as an inhibitor CI, and antimycin A [5 mM], which halts OXPHOS, was used to determine the residual oxygen consumption.

To analyze the data of mitochondrial respiration and H_2O_2 emission, DatLab Version 6.1.0.7 was used. Firstly, a section of the graph which corresponded to a steady state of mitochondrial respiration was chosen (figure 14). For mitochondrial respiration data 'O_2 flux per volume' value was chosen and the value of 'Amp slope' was chosen for H_2O_2 emission data.

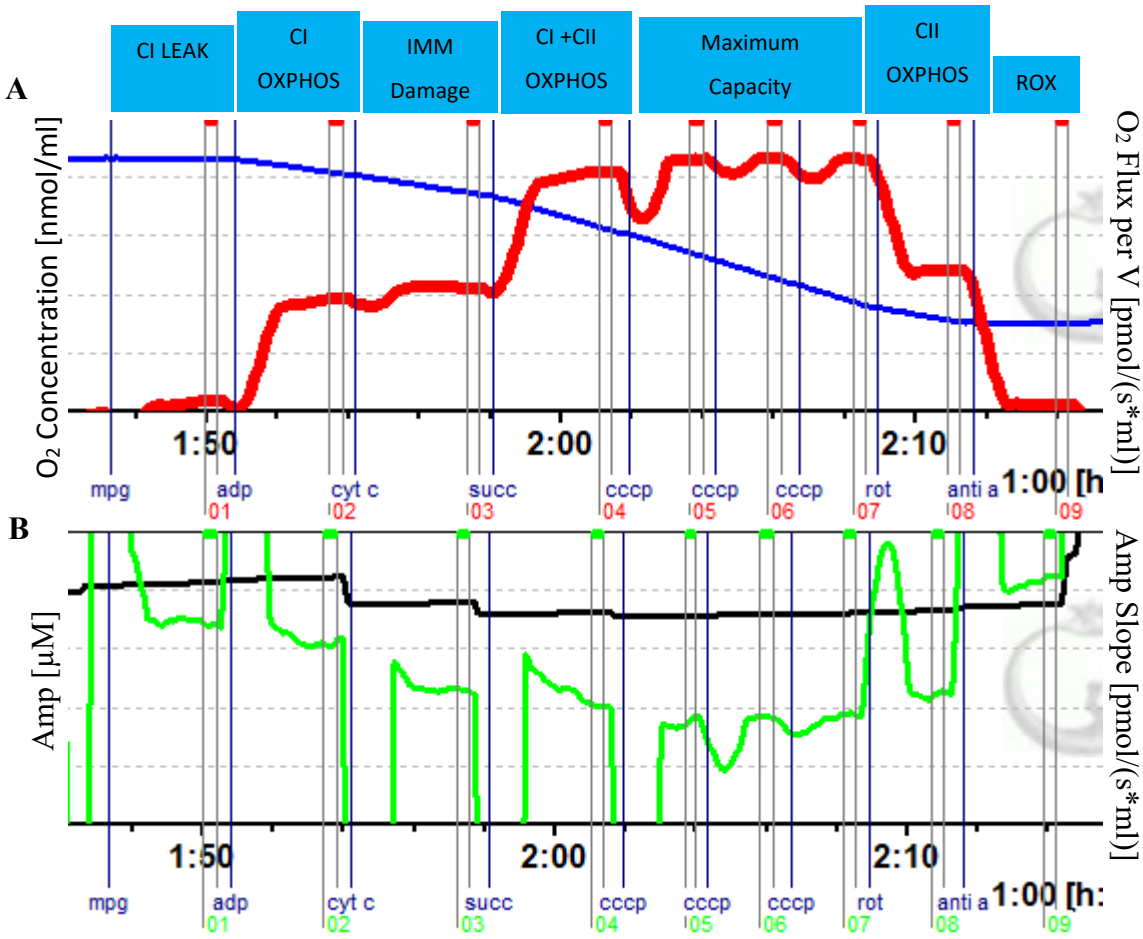

Figure 14. An example of a run of Oroboros O2k-FluoRespirometer high resolution respirometry (HRR). A) Simultaneous measurement of mitochondrial respiration with the sections whose statistical data were used in data analysis and B) hydrogen peroxide (H_2O_2) emission using Amplex® UltraRed and the sections whose statistical data were used in data analysis. Abbreviations: mpg: malate+pyruvate+glutamate. adp: adenosine diphosphate. cyt c: cytochrome C. succ: succinate. max cccp: maximum cccp (carbonyl cyanide m-chlorophenylhydrazone). rot: rotenone. anti a: antimycin A. CI LEAK: complex I leak [39]. CI OXPHOS: complex I oxidative phosphorylation [39]. CII OXPHOS: complex II oxidative phosphorylation [39]. CI+CII OXPHOS: complex I and II oxidative phosphorylation. ROX: residual oxygen consumption [39]. IMM: inner mitochondrial membrane.

3.3.3 H_2O_2 Emission

Following washing and calibration of the instrument, the lights of the chambers were turned off and the fluorometry sensors were plugged into the chambers. Then, the enzymes HRP [500 U/ml] and MnSOD [1.7 mg protein/ml; 3277 units/mg protein] were added followed by Amplex® UltraRed [10 mM], which is a probe of H_2O_2 and was used as the reagent of this

experiment to bind to H_2O_2. After that H_2O_2 [40 µM] was added in three steps to calibrate the level of H_2O_2 [40].

ROS are mostly produced in the CI and CIII of ETS in O_2^- form [41]. MnSOD catalyzes the conversion of these O_2^- to H_2O_2 [41]. HRP catalyzes the oxidation of Amplex® UltraRed to resorufin red fluorescent substance in the presence of H_2O_2 [41]. Although the concentration of H_2O_2 is maintained at low levels, increasing the signal of fluorescence linked to resorufin over time produces a slope associated with the reaction flux of H_2O_2 emission [41]. So, during the experiment the Amplex® UltraRed concentration decreases while the concentration of resorufin rises simultaneously [41] (figure 15).

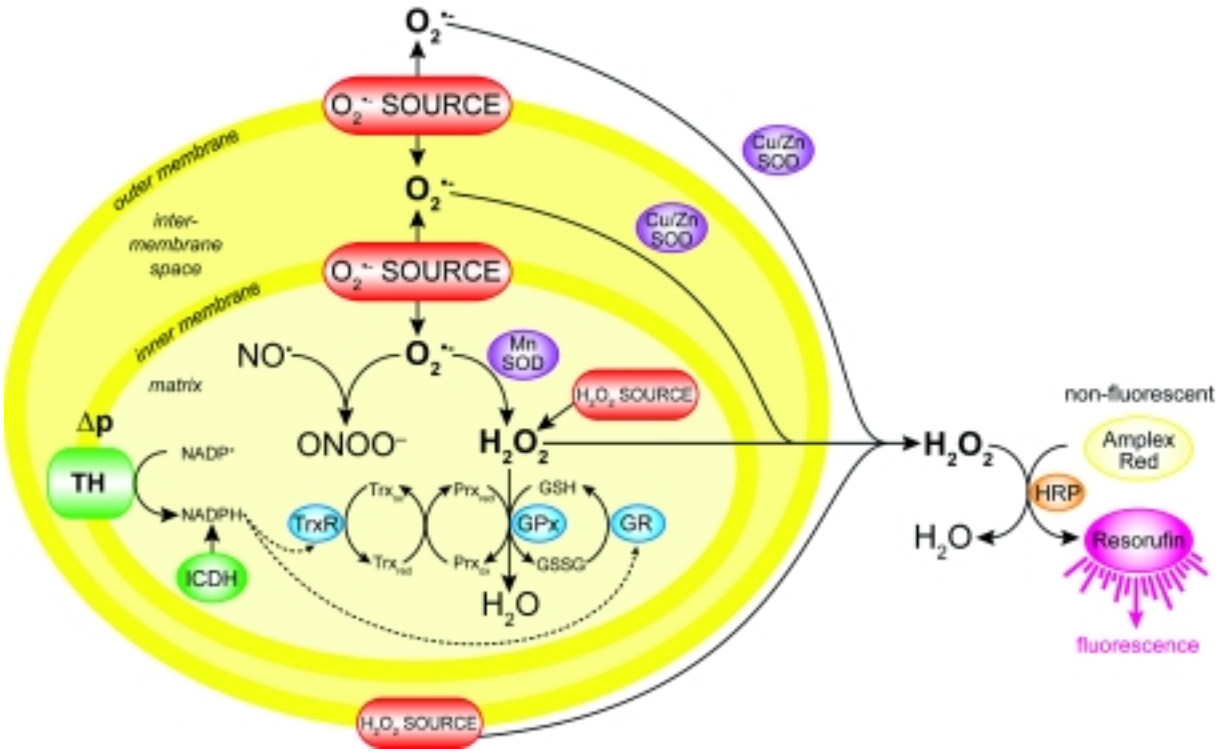

Figure 15. How hydrogen peroxide (H_2O_2) is produced in mitochondria. Superoxide anion ($O2^-$) is converted to H_2O_2 by superoxide dismutase (MnSOD), and horseradish peroxidase (HRP) converts H_2O_2 to water (H_2O) [42] [41]. HRP catalyzes the oxidation of Amplex® UltraRed to resorufin, a red fluorescent substance, in the presence of H_2O_2 [42] [41].

The H_2O_2 which was used in this calibration was made fresh daily. The H_2O_2 stock solution ((30% (w/w) in H_2O) (MW=34.01 gr/mol)) was diluted in 10 µM HCl in two steps. In the first step the H_2O_2 concentration was 10 mM and the final concentration was 40 µM.

To present the values for H_2O_2 emission in this thesis (section 4.4), these values were calculated as a ratio to the O_2 consumption data (mitochondrial respiration) using '(H_2O_2/(2*O_2 respiration rate))*100' [43] [44]. This ratio may provide an indication of the extent of the H_2O_2 production that could result in wasting of O_2.

3.4 Evaluation of Mitochondrial Content

There is no consensus within the field of an optimal factor to quantify the amount of mitochondria in the preparation to be assessed. Although this was not the main focus of this thesis, one of the minor aims was to also evaluate which factor provides the most accurate quantification of mitochondria that can be used to normalize both the mitochondrial respiration as well as the H_2O_2 emission for each experiment. Therefore, in the present study we have compared four methods to normalize the mitochondrial data to mitochondrial content, 1) by the tissue weight, 2) by the CS activity, 3) by the CS activity in the chamber, and finally 4) by the total protein content.

Tissue weight: A biopsy of 20-25 mg was used for the mitochondrial respiration and H_2O_2 emission experiments. In each experiment an appropriate volume of the tissue homogenate in accordance with the tissue weight was added to the chambers of the respirometer. If the tissue homogenate was very concentrated or the tissue piece was large, less volume of the tissue homogenate was added to the respirometer chambers, and vice versa.

Citrate synthase activity: CS is an enzyme in the mitochondria which has an important role in catalyzing the conversion of Acetyl CoA and oxaloacetate into citrate and CoA in the TCA cycle. After the cardiac homogenate was prepared, a sample of remaining homogenate was frozen for later analysis of CS activity. However, as mitochondrial respiration is being measured in the chamber, it was preferable to obtain the CS activity of the homogenate that was inside the chamber to provide the most accurate values of mitochondria that were respiring. Therefore, a sample (50 µl) was also taken from the respiration chamber after the homogenate was added and mixed in the MIR05, but prior to adding any substrates. Measurement of the CS activity of the homogenate in the chamber containing MIR05 had not previously been studied in depth at the Cardiovascular Research Group.

Triethanolamine-HCl (C_6H15NO_3-HCl) buffer ([0.1 M] (pH 8.0)) was made by diluting triethanolamine-HCl buffer ([0.5 M] (pH 8.0)) + EDTA ($C_{10}H_{16}N_2O_8$) [5 mM], which was used to remove unwanted ions, 1:5 in ddH_2O. Then, oxaloacetate was dissolved in this buffer to make oxaloacetate ([10 mM] (pH 8.0)). In this assay, DTNB (Ellman's reagent) ($C_{14}H_8N_2O_8S_2$) ([1.01 mM] (pH 8.1)) was used as a reagent to bind to CoA and produce TNB which yielded a yellow color. DTNB was dissolved in tris-HCl ($C_4H_{11}NO_3$-HCl) buffer ([1.0 M] (pH 8.1)) and protected from the light.

On the same day the standards of this assay were also prepared. CS from porcine heart (Sigma-Aldrich Chemie GmbH) was used as the external standard and a cardiac tissue homogenate from mouse and rat, prepared at the Cardiovascular Research group in 2016, was used as the internal standard. The external standard was diluted in two steps, first 1:500 and then 1:4, in tris-HCl ([0.1 M] (pH 7.0)) to reach a final dilution of 1:2000. The internal standard, however, was diluted 1:5 in tris-HCl ([0.1 M] (pH 7.0)).

Once the solutions and standards were made, the samples which were taken from the tissue homogenate were diluted 1:5 in tris-HCl ([0.1 M] (pH 7.0)) to be ready for the experiment while the chamber samples remained non-diluted. Then, a reaction mix was made which contained ddH_2O, oxaloacetate ($C_4H_4O_5$), Acetyl CoA ($C_{23}H_{38}N_7O_{17}P_3S$), and [10%] Triton X-100 ($C_{14}H_{22}O(C_2H_4O)_n$(n=9-10)) to lyse and permeabilize the membrane of the cells of the tissue homogenate. After that, the samples and standards were added to a microplate which was kept on ice. Finally, DTNB was added to the reaction mix as DTNB immediately started the reaction, and the complete reaction mix was added quickly to the microplate and the absorbance of UV by the yellow pigment was measured by a VersaMax™ Tunable Microplate Reader at an optical density of 412 nm for 2.5 minutes with 15-second intervals. The reaction rate of CS is used to determine the amount of mitochondria and can be used to normalize the mitochondrial respiration.

Total protein: The protein content of the cardiac tissue homogenate was also measured as another way to normalize the data. Firstly, 1:2 serial dilutions of a 1 mg/ml BSA, which was the standard solution of this experiment, were made in ddH_2O. Then, the samples and MiR05

were diluted 1:8 in ddH_2O. After adding the standards, samples, and buffer in a 96-well microplate, a Bio-Rad Protein Assay Dye Reagent (diluted 1:5 in ddH_2O), which was used as the reagent of this experiment, was added. Finally, a VersaMax™ Tunable Microplate Reader was used to measure protein content in the samples by measuring the absorbance of UV at optical densities of 450 and 590 nm.

Based on our assessment, the tissue weight, CS activity and total protein could be used to normalize for mitochondrial content. However, CS homogenate was chosen in the end because we think it gives us the most accurate number of mitochondria as opposed to other methods (figure 16). This was based on an evaluation where the same mitochondrial respiration state was compared using all the four normalization methods, and where the best correlation between respiration and the mitochondrial content was observed with CS activity in the tissue homogenate. In addition, the CS activity of the tissue homogenate was chosen due to several other limitations related to the other methods, such as the possibility that there could have been imprecisions in tissue weight measurements, the samples which were taken from the chamber for the CS assay were potentially too diluted, and protein concentration is the concentration of all of the proteins in the cardiac tissue homogenate and not exclusively to the mitochondria. In addition, there were indications that there was less variation when normalized to the CS homogenate.

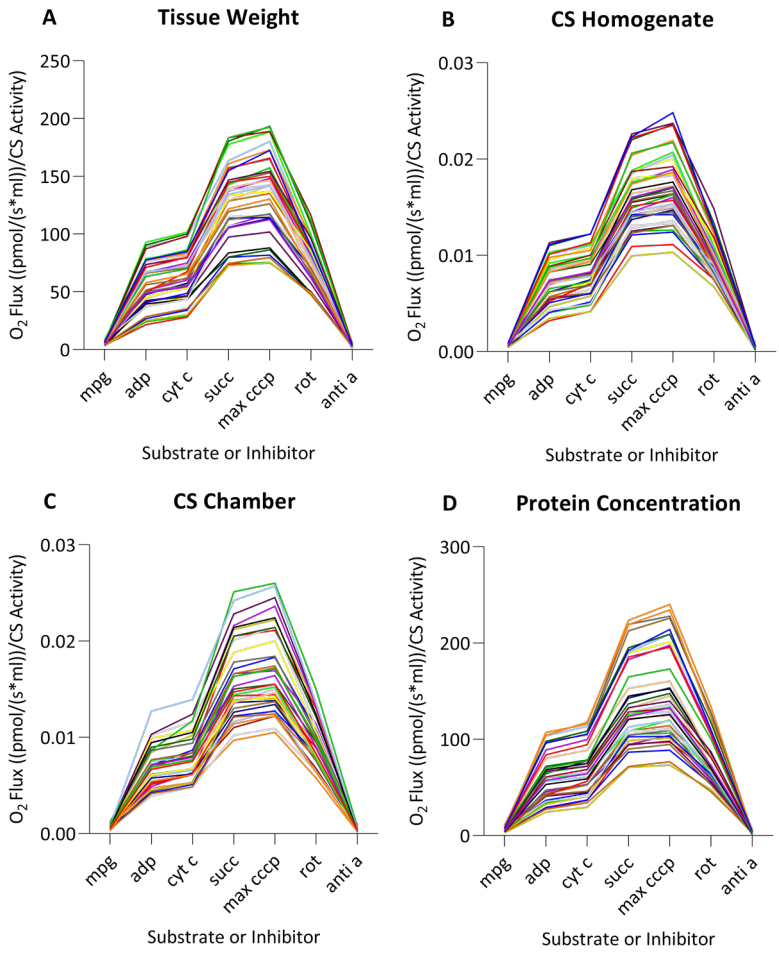

Figure 16. Four methods used to estimate the mitochondrial content for mitochondrial respiration data. CS: citrate synthase. mpg: malate+pyruvate+glutamate. adp: adenosine diphosphate. cyt c: cytochrome C. succ: succinate. max cccp: maximum cccp (Carbonyl Cyanide m-ChloroPhenylhydrazone). rot: rotenone. anti a: antimycin A.

3.5 Real time-Reverse Transcription Polymerase Chain Reaction (RT-PCR) to Measure mRNA Expression

RT-PCR is a common technique in molecular biology laboratory which is based on PCR and used to measure changes in mRNA expression. In this method, a target gene of a cDNA which is synthesized from an RNA is amplified and this amplification can be observed over time.

3.5.1 RNA Stabilization

To preserve RNA, the cardiac tissue biopsies were kept in an RNA Stabilization Reagent, RNAlater® (Qiagen), for approximately 24 hours. Prior to being put in this reagent, the cardiac tissue biopsies were weighed to find out how much tissue would be needed to have an optimal concentration of total RNA to make the cDNA.

3.5.2 RNA Isolation

To isolate the RNA, an RNAeasy fibrous tissue mini kit (Qiagen) was used. Firstly, to lyse the tissue and denature RNases, the tissue was disrupted and homogenized in buffer RLT containing 1% β-ME by using a Qiagen TissueLyser LT. Next, proteinase K enzyme (diluted 1:60 in RNase-free H_2O) was added to the lysate to digest ribonucleases and ribosomal proteins, and the samples were incubated at 55°C for 10 minutes. After centrifugation at 10,000 g for 3 minutes, the supernatants were transferred to new tubes and 0.5 volumes absolute [100%] ethanol (C_2H_5OH) was added for precipitation of the RNA. Then, the solution was transferred to an RNeasy Mini column and the flow-through was discarded after centrifugation at 8000 g for 15 seconds. In the next step, buffer RW1 was added to the RNeasy column to wash the silica membrane and remove unwanted biomolecules including carbohydrates and proteins. After centrifugation at 8000 g for 15 seconds and discarding the flow-through, DNase (diluted 1:8 in buffer RDD) was added to RNeasy membrane in order to digest DNA and keep RNA bound to the column, and the samples were incubated at room temperature for 15 minutes. Next, the samples were washed again with buffer RW1 and the flow-through was discarded after centrifuging at 8000 g for 15 seconds. Then, the column was washed with buffer RPE (diluted 1:5 in absolute ethanol) to remove the leftovers of the salts of the previous buffers from the column and the samples were centrifuged at 8000 g for 15 seconds. After discarding the flow-through the column was again washed with buffer RPE and samples were centrifuged at 8000 g for 2 minutes. In the end, the RNeasy column was placed in a new tube and RNase-free H_2O was added to elute the RNA and the samples were centrifuged at 8000 g for 1 minute.

A NanoDrop™ 2000 spectrophotometer (Thermo Fisher SCIENTIFIC) was used to measure RNA content in the samples by measuring the absorbance of UV at optical densities of 260 and 280 nm.

3.5.3 cDNA (Complementary DNA) Synthesis; Reverse Transcription

To determine the cDNA, a High-Capacity cDNA Reverse Transcription Kit (Thermo Fisher SCIENTIFIC) was used. Firstly, it was calculated how much of the isolated RNA solution should be mixed with RNase-free H_2O in the cDNA tube to have an RNA concentration of 1000 ng/sample. Then, two cDNA mixtures were made for this experiment. One of them included 10X RT buffer, 10X RT random primers, 25X dNTP mix [100mM], MultiScribe® Reverse Transcriptase [50U/µL], and RNase-free H_2O. The other mixture which was used for non-reverse transcription control samples did not include the reverse transcriptase enzyme. Next, these mixtures were added to their corresponding RNA sample tubes. After 10 minutes incubation at 25°C, the samples were incubated for 2 hours at 37°C. After that, the samples were incubated at 95°C for 5 minutes, cooled down and spun. In the end, RNase-free H_2O was added to the samples to make them ready for gene expression analyses. A cDNA pool, which was a mixture of all the samples, was also made.

3.5.4 Primer Optimization

As they had not been used at the Cardiovascular Research Group previously, eight new primers (*glutathione reductase* (*grs*), *glutathione synthetase* (*gss*), *glutaredoxin 2* (*grx2*), *hypoxia induced gene domain 1a* (*higd1a*), *hypoxia induced gene domain 2a* (*higd2a*), *mitofusin 1* (*mfn1*), *mitofusin 2* (*mfn2*), *optic atrophy 1* (*opa1*)) (appendix IV apart from *glutathione peroxidase 3* (*gpx3*) which was already available at the cardiovascular research group) needed to be optimized to find out the optimal concentration to be used in RT-PCR experiments. Working solutions of 10 µM concentrations were first made from 200 µM stock solutions of these primers. Then, the reverse and forward primers were diluted in RNase-free H_2O in four different concentrations: 100 nM, 200 nM, 400 nM, and 800 nM. Two master mixes were also made. One included a FastStart Essential DNA Green Master (Roche Molecular Systems, Inc.), cDNA, and RNase-free H_2O while the other one did not include the

cDNA and was used as the non-reverse transcription control. After that, the samples and mixes were added in a 96-well PCR plate, spun, and finally read by LightCycler® 96 Instrument (Roche Molecular Systems, Inc.).

3.5.5 Gene Quantification

To quantify the expression of housekeeping and target genes RT-PCR experiments were performed. In these experiments, firstly 1:5 serial dilutions from the cDNA pool were made to be used as standards. A master mix to quantify the reference and target genes was also made and included a FastStart Essential DNA Green Master, forward and reverse primers in accordance with the reference or target gene, and RNase-free H_2O. Then, this was mixed with the cDNA samples in a 96-well qPCR plate. RNase-free H_2O was also used as a negative control. After that, the plate was spun and read by a LightCycler® 96.

3.5.6 Data Analysis

'GeNorm' 3.4 [45] was used to find the most stable housekeeping gene within five housekeeping genes analyzed by LightCycler® 96 (cyclophilin, HPRT, GAPDH, HMBS, and SDHA) based on the standard deviation of logarithmically transformed expression ratios and efficiency adjusted quantification cycle (Cq) value for each sample.

The 'GeNorm' software automatically calculated the stability of a gene (M value) in a set of samples. Genes with the lowest M values were the most stable ones. In addition, it gave the optimal number of housekeeping genes to be used for normalization.

The most stable housekeeping genes were found to be cyclophilin, HPRT, GAPDH, and HMBS. After that, the geomean of these four housekeeping genes was calculated and used to normalize the data of the target genes. Finally, the housekeeping gene normalized target genes data were normalized to the LP-perfused hearts, that was chosen as the control group in this data set.

3.6 Analysis of Reduced (GSH) and Oxidized (GSSG) Glutathione Levels Using Liquid Chromatography Tandem Mass Spectrometry (LC MS/MS)

Following heart perfusion, cardiac tissue samples were prepared for later analysis of GSH and GSSG. Weighed cardiac tissue biopsies (30-50 mg) were placed in 500 µL of washing buffer (appendix V) and 250 µL NEM (appendix V), prior to homogenization by sonication. NEM was prepared so as to avoid auto-oxidation of GSH [46]. Internal standards for GSH and GSSG that contained isotope-labelled GSH ((Glycine-13C2, 15N)-Glutathione, Cambridge Isotope Laboratories) (appendix VI) were prepared fresh each day and were mixed well to the sonicated tissue. Protein denaturization occurred by the addition of trichloroacetic acid (CCl_3COOH) [8 M] and gentle mixing for 1 minute. Dichloromethane (CH_2Cl_2) was then added to extract NEM. To obtain the aqueous phase and separate the NEM containing dichloromethane from the sample as well as the excess tissue, the samples were then centrifuged for 5 minutes at 3200 rpm at room temperature. Then, the aqueous phase was transferred to Eppendorf tubes and centrifuged for 10 minutes at 14000 rpm at 4°C to ensure that all dichloromethane was removed. The dichloromethane-free liquid was then transferred to a new tube and stored at -20°C.

Prior to analysis, GSH and GSSG standards at known concentrations were determined (Appendices VII and VIII). Due to the differences in concentration levels between GSH and GSSG, and because GSH is normally in much higher concentrations than GSSG, samples were prepared as diluted (1:20) and non-diluted in MS vials (Waters©). Thus, GSH levels were determined in diluted samples whereas GSSG levels were determined in non-diluted samples following measurement using LC MS/MS.

LC-MS/MS: In this technique the molecular mass of a protein sample is determined [47]. The proteins are first broken down into small peptides by trypsin and then separated by liquid chromatography [47]. After that, in the mass spectrometer (MS) the peptides are quantified based on their mass to charge ratio (m/z) [47]. Further in MS/MS, the quantified peptides of

MS are quantified [47]. Analyses using LC-MS/MS were performed by another researcher, including data analyses. Therefore, I will not go into further details regarding this technique.

3.7 Non-esterified Fatty Acid (NEFA) Determination in Bovine Serum Albumin and Cardiac Perfusion Buffer

To ensure that the BSA used for the present study did not contain excessive fatty acids and also to measure the final palmitate (fatty acid) concentration in the buffer to perfuse the hearts, the quantity of NEFA was determined in new BSA and in the perfusion buffer using a NEFA-HR(2) (FUJIFILM Medical Systems U.S.A. Inc.).

In this method, coexisting with CoA and adenosine 5-triphosphate disodium salt (ATP), Acyl-CoA synthetase (ACA) converts NEFA of the samples to Acyl-CoA, AMP, and pyrophosphoric acid (PPi). Then, Acyl-CoA oxidase (ACOD) oxidizes the Acyl-CoA to produce 2,3-trans-Enoyl-CoA and H_2O_2. After that, in a quantitative oxidation condensation with 3-Methyl-N-Ethyl-N-(β-Hydroxyethyl)-Aniline (MEHA) and 4-amino-antipyrine (4-AA) while peroxidase (POD) is present, the H_2O_2 produces a blue purple pigment. Next, the absorbance of UV by this blue purple color is measured by a spectrophotometer at an optical density of 540 nm to determine the concentration of NEFA in the samples.

The samples, R1 set reagent (appendix IX), and standards with known concentrations (including BSA (external standard) and control serum (internal standard)), were pipetted in a microplate. After 10 minutes incubation at 37°C, R2 set reagent (appendix IX) was added, followed by shaking and another 10 minutes incubation at 37°C. After that, any potential bubbles were removed and after a final 10 minutes incubation, the microplate was read by a VersaMax™ Microplate Reader.

3.8 Protein S-Glutathionylation Determination Using Western Blotting

3.8.1 Sample Preparation

Firstly, samples for western blot were prepared from approximately 50 mg of frozen cardiac tissue. The tissue was immersed in 250 µl of homogenization buffer (RIPA buffer) (appendix

X) in a tube with a metal bead. Next, the tissue was lysed using a Qiagen TissueLyser LT for 2 minutes at 40 Hz. Then, samples were centrifuged at 15000 rpm at 4°C for 20 minutes. The pellet was discarded, and supernatant was used to determine the protein concentration by detergent compatible (DC) assay.

In the DC assay, serial dilutions of 1 mg/ml BSA were used as the standards. The samples were also diluted 5, 10, and 20 times. Reagent A (an alkaline copper tartrate solution) was mixed with reagent S (a surfactant solution) to make an A^i. The samples and standards were added in a 96-well plate then A^i and reagent B (a dilute Folin Reagent) were added to them. The plate was placed in a shaker for 15 minutes and at an optical density of 690 nm the protein concentration was measured by a VersaMax™ Microplate Reader.

Samples were prepared using 2x Laemmli Sample Buffer (1:2). In addition, negative controls containing 4% (v/v) β-ME, which is a reducing agent that reduces disulfide bonds, were included. As the GSSG has been reduced to GSH in the negative control samples there is no GSSG for the anti-PSSG antibody to bind to and thus no bands should be seen. All the samples were boiled at 95°C for 5 minutes.

3.8.2 Making Acrylamide Gels

To measure protein S-glutathionylation, 8% acrylamide gels were prepared (appendix XI). During separating gel polymerization, 50% isopropanol was added on top of the gel to obtain a flat interface. Approximately 30 minutes later the isopropanol was removed, the 5% acrylamide stacking gel (appendix XII) was added and combs were set in the stacking gel. The stacking gel required approximately 30 minutes to polymerize.

3.8.3 SDS-PAGE (sodium dodecyl sulphate–polyacrylamide gel electrophoresis) and Immunoblotting

The samples were loaded to the gel with a concentration of 30 µg/lane. Precision Plus Protein™ Standard was used as a ladder for the acrylamide gel and MagicMark™ XP Western Protein Standard was used as a ladder for the nitrocellulose membrane. The gel was placed in running buffer (appendix XIII) for approximately 75 minutes at 120V voltage. This allowed SDS to

denature and bind to proteins. The negatively charged proteins migrated through the gel from the negative to the positively charged electrode until they reached the bottom of the gel. Then, the gel was transferred to a nitrocellulose membrane with 0.2 µm pore size in a wet transfer. The transfer was performed at 100V voltage for 60 minutes using an ice-cold transfer buffer containing methanol (appendix XIV) to remove SDS. Then, ponceau stain (appendix XV), which binds to proteins, was used to visualize the protein bands to confirm the transfer prior to doing the blocking step. After that, the membrane was washed with TBS-T (appendix XVI) to remove the ponceau stain and transferred to a blocking buffer (5% blotting-grade blocker (nonfat dry milk) dissolved in TBS-T). This step was to get rid of the non-specific bindings and the membrane was incubated in blocking bluffer on a shaking table for 60 minutes. The membrane was washed 3 times with TBS-T, each time for 5 minutes, and put in an anti-PSSG primary antibody solution (anti glutathione monoclonal antibody [1 mg/ml] (ViroGen©) dissolved 1:500 in TBS-T containing 5% BSA) on a shaking table at 4°C overnight. The next day, the membrane was placed in an anti-mouse secondary antibody solution (goat primary antibody to Ms IgG (HRP) [0.5 mg/ml] (Abcam©) dissolved 1:5000 in TBS-T containing 5% blotting-grade blocker (nonfat dry milk)) on a shaking table at room temperature for 60 minutes. After washing 3 times with TBS-T, each time for 5 minutes, the membrane was ready for imaging.

The ImageQuant Las 4000 luminescent image analyzer was used for imaging the membrane. Prior to performing the imaging, 'Clarity™ Western ECL Substrate peroxide solution' was mixed equally with 'Clarity™ Western ECL substrate luminol/enhancer solution' and poured on the membrane. Finally, the imaging was done in using high resolution precision mode for 4 minutes of exposure time. Fiji was used to analyze the blots of western blotting experiments [48].

3.9 Statistical Analysis

GraphPad Prism version 8.4.3 for Windows, GraphPad Software, San Diego, California USA, was used to statistically analyze the data and make the graphs of this project. One-Way ANOVA followed by Holm-Sidak multiple comparisons test was performed to compare the

statistical significance within the groups. All data is presented as means +/- SD (standard deviation). To have a normal (Gaussian) distribution of the data, in which the highest and lowest values in a group of samples are distributed symmetrically to the mean, the values which could not pass Shapiro-Wilk normality test where $p<0.05$, were transformed reciprocally by being recalculated to Y=1/Y. Outliers were also removed when applicable.

4 Results

4.1 Ischemia-reperfusion and Diamide significantly Alter the Cardiac Function

Although the elevated levels of palmitate did not alter the cardiac function in the working heart perfusion system, the function of the hearts which were exposed to IR and diamide is significantly impaired, as demonstrated in figure 17. In the hearts treated with the LP the cardiac output (coronary flow + aortic flow) is drastically dropped following IR and diamide treatments compared to LP (8.69 ± 1.77 and 4.92 ± 1.73 vs. 14.81 ± 1.44, ml/min) (figure 17A). In the hearts which were exposed to the HP, however, depressed cardiac output was demonstrated after diamide treatment in comparison with HP (5.40 ± 2.72 vs. 12.25 ± 3.77, ml/min) but was not significantly altered following IR (figure 17A).

The cardiac power (cardiac output * heart rate) was also significantly altered by IR and diamide in both LP and HP treatments (2624 ± 516.8 and 1665 ± 515.5 vs. 5402 ± 1178, ml/min * beats per minute) and (1817 ± 789.2 and 1968 ± 1127 vs. 4449 ± 2091, ml/min * beats per minute) (figure 17B).

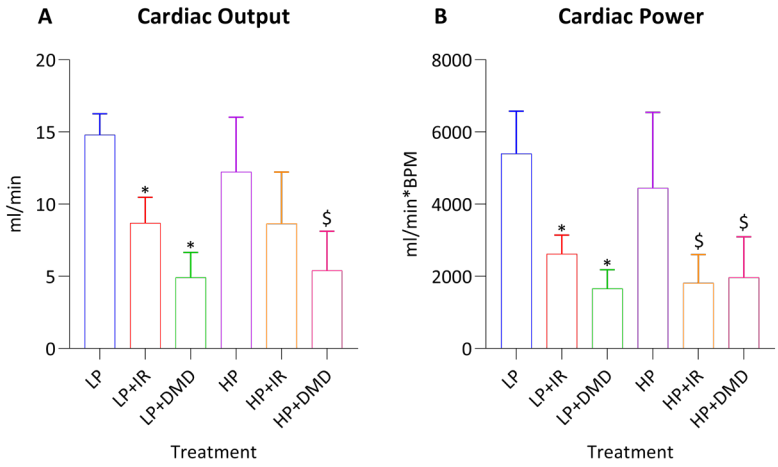

Figure 17. Assessment of A) cardiac output and B) cardiac power in isolated working hearts. N=5-8. * $p<0.05$ vs. LP. $ $p<0.05$ vs. HP. One-way ANOVA and Holm-Sidak multiple comparison tests were used for statistical analysis. Data are represented as means ± SD. IR: ischemia-reperfusion. LP: low palmitate. LP+IR: low palmitate plus ischemia-reperfusion. LP+DMD: low palmitate plus diamide. HP: high palmitate. HP+IR: high palmitate plus ischemia-reperfusion. HP+DMD: high palmitate plus diamide. BMP: beats per minute.

Both IR and diamide treatment reduced the aortic flow, in comparison with LP and HP controls. This supports other findings that the concentration of palmitate did not have any additional effects on cardiac function during either treatment. No significant difference in coronary flow, aortic pressure or heart rate was found between the groups (table 1).

Table 1. Cardiac function in isolated perfused working hearts. N=5-8. * p<0.05 vs. LP. $ p<0.05 vs. HP. One-way ANOVA and Holm-Sidak multiple comparison tests were used for statistical analysis. Data are represented as means ± SD. IR: ischemia-reperfusion. LP: low palmitate. LP+IR: low palmitate plus ischemia-reperfusion. LP+DMD: low palmitate plus diamide. HP: high palmitate. HP+IR: high palmitate plus ischemia-reperfusion. HP+DMD: high palmitate plus diamide. BMP: beats per minute.

Treatment	LP	LP+IR	LP+DMD	HP	HP+IR	HP+DMD
Coronary Flow (ml/min)	2.75 ± 0.43	2.12 ± 0.18	3.36 ± 0.34	2.57 ± 0.55	2.44 ± 0.37	2.52 ± 0.86
Aortic Pressure (mmHg)	51.31 ± 3.09	52.78 ± 1.77	51.32 ± 2.07	51.93 ± 2.57	45.96 ± 12.77	49.14 ± 1.87
Aortic Flow (ml/min)	12.19 ± 1.38	5.60 ± 2.55 *	1.52 ± 1.61 *	9.67 ± 3.34	5.00 ± 2.09 $	2.38 ± 2.06 $
Heart Rate (BMP)	387.5 ± 12.61	310.0 ± 53.10	341.8 ± 14.80	374.3 ± 44.67	256.4 ± 90.01	353.7 ± 48.68

4.2 GSH/GSSG is Significantly Altered by Diamide

Neither palmitate nor IR demonstrated significant effects in altering GSH/GSSG and GSH content. But diamide had profound effects on GSH, GSSG, and GSH/GSSG. GSH content was significantly decreased when the heart was exposed to diamide in both low (1083 ± 267.7 vs. 3874 ± 808.2, µmol/mg wet weight) and high concentrations of palmitate (1166 ± 387.6 vs. 3553 ± 350.8, µmol/mg wet weight) (figure 18A).

Unlike IR, palmitate and diamide showed significant effects in altering GSSG content. As expected, a reverse trend was seen with the GSSG levels as compared to GSH, where diamide increased the GSSG content significantly. Diamide treatment resulted in significantly increased GSSG in hearts perfused with LP (118.1 ± 13.99 vs. 4.25 ± 0.9056, µmol/mg wet

weight) (Figure 18B). In hearts perfused with HP, GSSG was also increased following diamide treatment (70.28 ± 19.07 vs. 4.23 ± 1.30, µmol/mg wet weight) (Figure 18B). However, a significant decrease of GSSG is apparent in the hearts perfused with high as compared to low palmitate following diamide treatment. This could be because of potential contribution of palmitate in replenishing GSH which can lead to reducing GSSG.

As opposed to palmitate and IR, diamide dramatically decreased GSH/GSSG for both low (9.27 ± 2.67 vs. 912.6 ± 231.0, µmol/mg wet weight) and high palmitate perfused hearts (16.92 ± 5.13 vs. 918.1 ± 273.4, µmol/mg wet weight) (figure 18C). Although GSH/GSSG tends to be higher in the hearts perfused with HP+DMD compared to LP+DMD, this was not found to be significantly different (p=0.99).

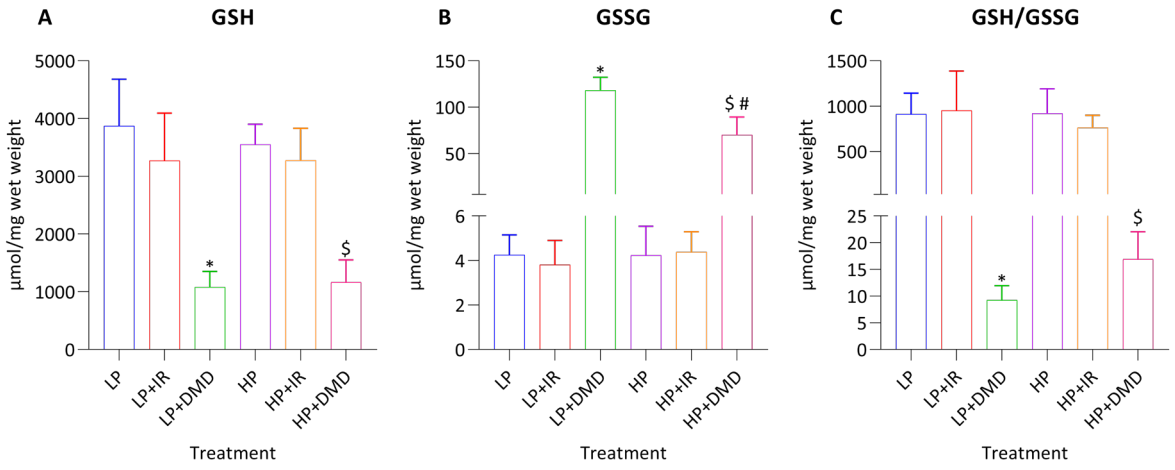

Figure 18. Glutathione levels in hearts perfused with low and high palmitate, following ischemia-reperfusion and diamide treatment. A) reduced glutathione, GSH, B) oxidized glutathione, GSSG and C) the ratio of GSH/GSSG as an indicator of the redox environment were determined. N=6-8. * p<0.05 vs. LP. $ p<0.05 vs. HP. # p<0.05 vs. LP+DMD. One-way ANOVA and Holm-Sidak multiple comparison tests were used for statistical analysis. Data are represented as means ± SD. IR: ischemia-reperfusion. LP: low palmitate. LP+IR: low palmitate plus ischemia-reperfusion. LP+DMD: low palmitate plus diamide. HP: high palmitate. HP+IR: high palmitate plus ischemia-reperfusion. HP+DMD: high palmitate plus diamide. GSH: glutathione. GSSG: glutathione disulfide.

4.3 Diamide Significantly Depresses Mitochondrial Respiration

As described in the Methods (Section 3.4) the mitochondrial respiration data was normalized to the amount of mitochondria in the homogenate. As there are many methods to estimate

the mitochondrial content, four different methods were tested to assess how the normalization could alter the results. These were: the weight of the tissue biopsy, the activity of CS in the cardiac tissue homogenate, the protein concentration in each sample, and the CS activity in the samples taken from chamber of the O2k (figure 16). However, the CS activity measured in samples from the cardiac homogenate was chosen to normalize all respiration and H_2O_2 emission data. This was measured by a CS activity assay.

Although there was a trend towards lowered CI-associated proton leak (CI LEAK) following IR and diamide treatment, there were no significant differences between the groups (figure 19A). In CI-associated coupled respiration (CI OXPHOS) the mitochondrial respiration was unchanged in hearts perfused with HP, nor did IR have any effects. CI OXPHOS was however significantly decreased following diamide treatment in both LP and HP perfused hearts (0.0043 ± 0.0012 vs. 0.0082 ± 0.0014, O_2 Flux ((pmol/(s*ml))/CS Activity)) and (0.0044 ± 0.0012 vs. 0.0067 ± 0.0015, O_2 Flux ((pmol/(s*ml))/CS Activity)) (figure 19B). Although, CI OXPHOS tends to be lower in mitochondria from HP-perfused hearts, this was not found to be significant.

Diamide lowered respiration for CI&CII-associated coupled respiration (CI+CII OXPHOS) in mitochondria from LP-perfused hearts (0.012 ± 0.0032 vs. 0.018 ± 0.0028, O_2 Flux ((pmol/(s*ml))/CS Activity)) but not from HP-perfused hearts, and there were no other differences between the groups (Figure 19C). During succinate-associated respiration with CI inhibition (CII OXPHOS) diamide treatment resulted in lower respiration for LP-perfused hearts (0.0048 ± 0.0014 vs. 0.0078 ± 0.0013, O_2 Flux ((pmol/(s*ml))/CS Activity)) (figure 19D).

In agreement, titrated CCCP-induced maximal respiration (where there is maximum electron transfer) of mitochondrial respiration was significantly reduced in LP-perfused hearts following diamide (0.013 ± 0.0032 vs. 0.019 ± 0.0032, O_2 Flux ((pmol/(s*ml))/CS Activity)) (figure 19E).

To further assess the efficiency of OXPHOS, these values were calculated using the respiration conditions demonstrated above. Calculation of the OXPHOS coupling efficiency (OCE), which is the ratio of consumed oxygen associated with ATP production and LEAK respiration (1-(CI

LEAK/CI OXPHOS)) [49], demonstrated that diamide lowered OCE in both LP and HP-perfused hearts (0.87 ± 0.021 vs. 0.91 ± 0.0097, O_2 Flux ((pmol/(s*ml))/CS Activity)) and (0.86 ± 0.0087 vs. 0.91 ± 0.016, O_2 Flux ((pmol/(s*ml))/CS Activity)) (figure 19F).

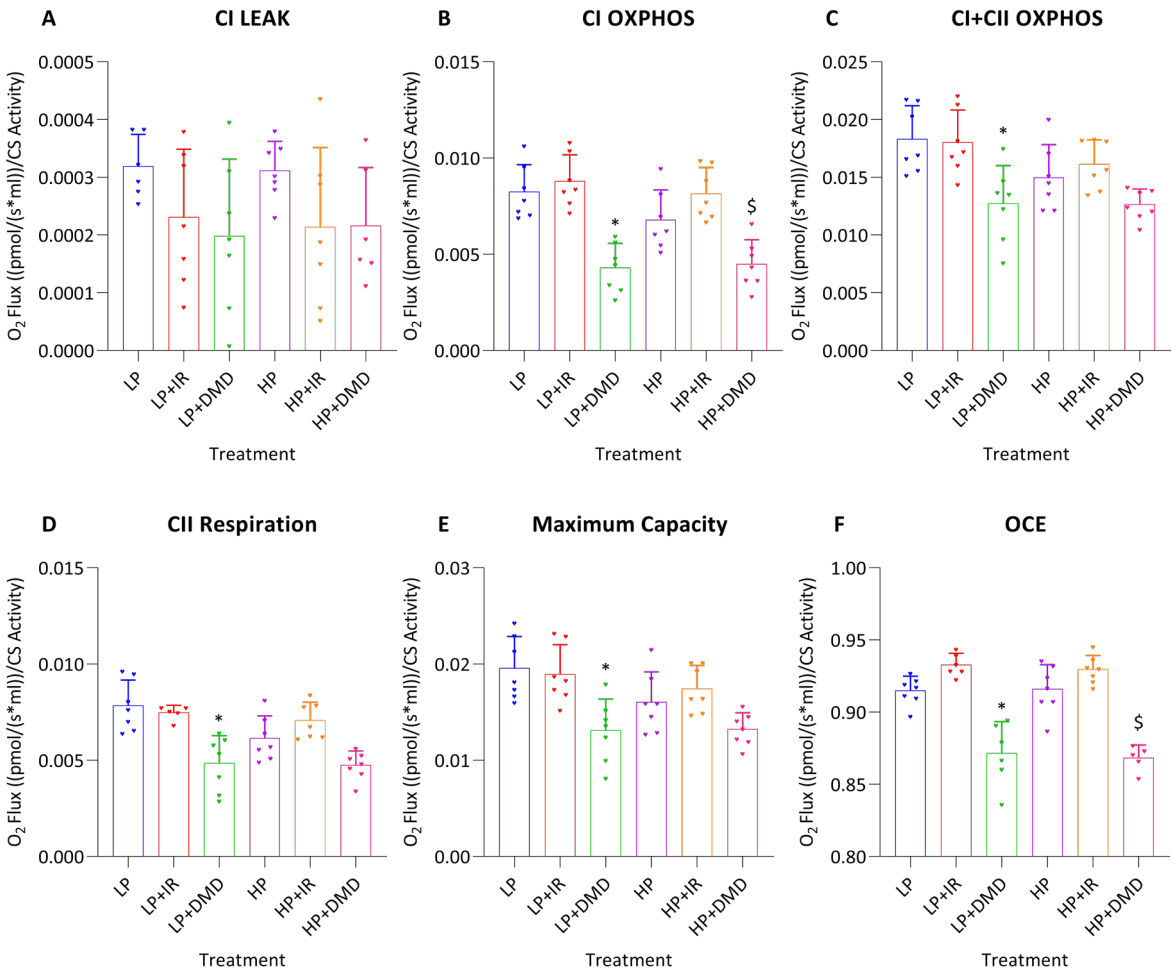

Figure 19. Mitochondrial respiration in cardiac homogenate from isolated hearts perfused with low and high palmitate following ischemia-reperfusion or diamide treatment. N=5-7. * p<0.05 vs. LP. $ p<0.05 vs. HP. One-way ANOVA and Holm-Sidak multiple comparison tests were used for statistical analysis. Data are represented as means ± SD. IR: ischemia-reperfusion. LP: low palmitate. LP+IR: low palmitate plus ischemia-reperfusion. LP+DMD: low palmitate plus diamide. HP: high palmitate. HP+IR: high palmitate plus ischemia-reperfusion. HP+DMD: high palmitate plus diamide. CI: complex I. CII: complex II. OXPHOS: oxidative phosphorylation. OCE: OXPHOS coupling efficiency.

4.4 Diamide Significantly Increases H_2O_2 Emission

Figure 20 demonstrates that overall, perfused hearts treated with diamide significantly increased the emission of H_2O_2 in all the evaluated states of mitochondrial respiration apart from CI LEAK (figure 20A). These results are presented as a ratio of H_2O_2 emission and O_2 consumption (mitochondrial respiration).

Although H_2O_2 production tends to be higher during CI LEAK following IR and diamide treatment, these differences were not significant (figure 20A). In the CI OXPHOS state of mitochondrial respiration, the emission of H_2O_2/O_2 consumption was significantly increased following diamide treatment in both LP and HP perfused hearts (0.032 ± 0.009 vs. 0.016 ± 0.0014, O_2 Consumption Towards H_2O_2 Production (%)) and (0.031 ± 0.0079 vs. 0.016 ± 0.0029, O_2 Consumption Towards H_2O_2 Production (%)) (figure 20B). However, there were no differences found following IR or by HP-perfusion alone.

H_2O_2 emission/O_2 consumption was also markedly increased in CI+CII OXPHOS state of mitochondrial respiration in LP and HP-perfused hearts following diamide treatment (0.0059 ± 0.0014 vs. 0.0039 ± 0.00026, O_2 Consumption Towards H_2O_2 Production (%)) and (0.0065 ± 0.0010 vs. 0.0048 ± 0.00066, O_2 Consumption Towards H_2O_2 Production (%)) (figure 20C).

During the CCCP-induced maximal capacity of mitochondrial respiration, H_2O_2 emission/O_2 consumption was also increased in LP and HP-perfused hearts (0.0067 ± 0.0014 vs. 0.0039 ± 0.00062, O_2 Consumption Towards H_2O_2 Production (%)),(0.0064 ± 0.0013 vs. 0.0042 ± 0.00056, O_2 Consumption Towards H_2O_2 Production (%)) following diamide treatment (figure 20D).

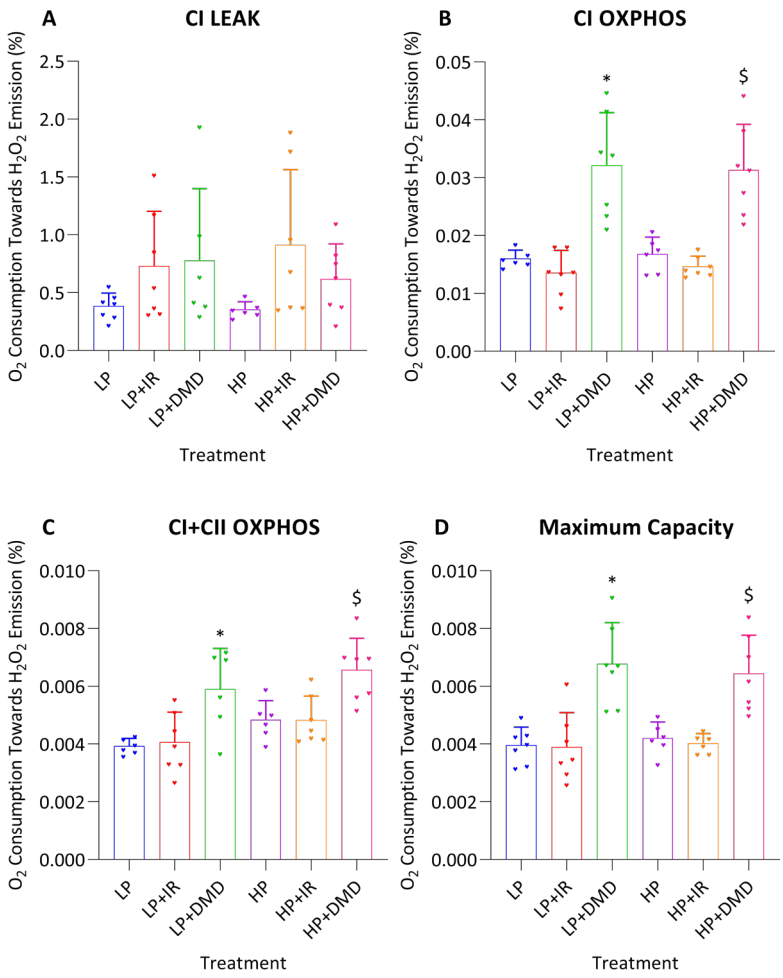

Figure 20. H_2O_2 emission during mitochondrial respiration in hearts perfused with low and high palmitate following ischemia-reperfusion or diamide treatment. N=6-7. * p<0.05 vs. LP. $ p<0.05 vs. HP. One-way ANOVA and Holm-Sidak multiple comparison tests were used for statistical analysis. Data are represented as means ± SD. IR: ischemia-reperfusion. LP: low palmitate. LP+IR: low palmitate plus ischemia-reperfusion. LP+DMD: low palmitate plus diamide. HP: high palmitate. HP+IR: high palmitate plus ischemia-reperfusion. HP+DMD: high palmitate plus diamide. CI: complex I. CII: complex II. OXPHOS: oxidative phosphorylation.

4.5 Diamide Alters the Expression of Two Target Genes Related to GSH Synthesis

In the present thesis, mRNA expression of several genes related to glutathione redox as well as mitochondrial fusion were examined. Interestingly, there were some differences in translational changes between the hearts perfused with LP and HP. These are '*glutathione reductase*' (*grs*) and '*glutathione synthetase*' (*gss*) and their expression was significantly

increased in LP+DMD and HP+DMD respectively. The expression of '*glutathione reductase*' (*grs*) was markedly increased in the hearts perfused with LP following diamide treatment (0.31 ± 0.038 vs. 0.2 ± 0.036, normalized to reference gene), but not IR (figure 21B). However, there were no changes in mRNA levels in the hearts perfused with HP. In addition, increased expression of '*glutathione synthetase*' (*gss*) was shown in hearts perfused with HP following diamide treatment (0.075 ± 0.005 vs. 0.061 ± 0.004, normalized to reference gene), but not by IR or HP alone (figure 21D). There were no significant changes in either '*glutathione peroxidase 3*' (*gpx3*) or '*glutaredoxin 2*' (*grx2*) mRNA expression (figures 21 A and C) for any of the groups.

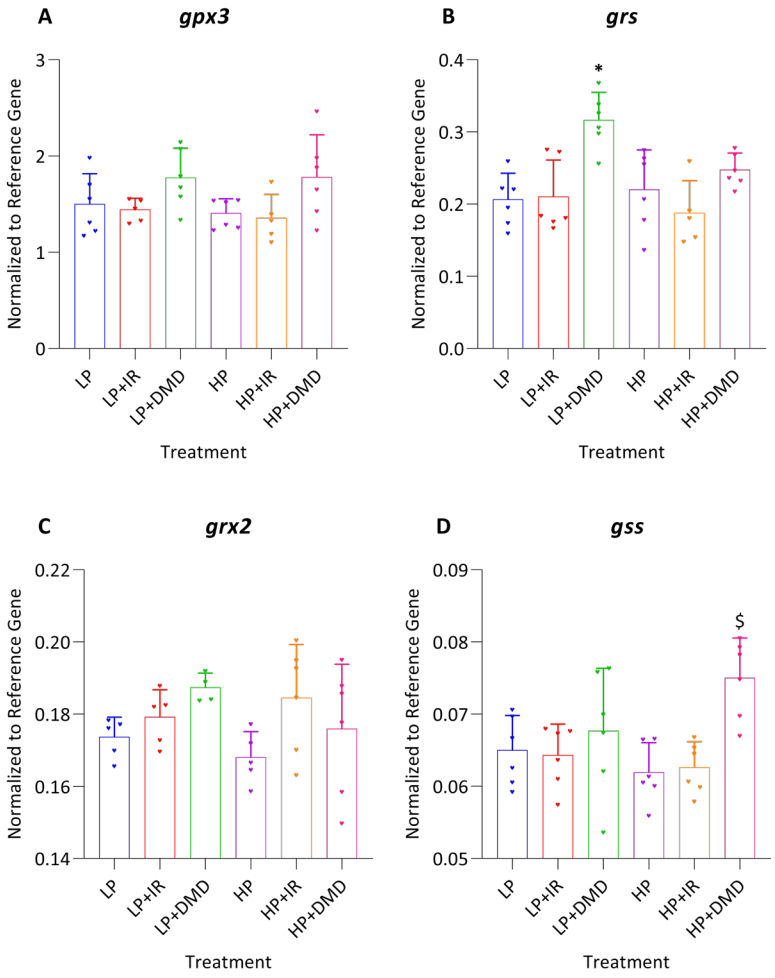

Figure 21. Diamide alters the expression of two glutathione-related genes, '*glutathione reductase*' (*grs*) and '*glutathione synthetase*' (*gss*), in the isolated perfused mouse heart. N=4-6. * p<0.05 vs. LP. $ p<0.05 vs. HP. One-way ANOVA and Holm-Sidak multiple comparison tests were used for statistical analysis. Data are

represented as means ± SD. IR: ischemia-reperfusion. LP: low palmitate. LP+IR: low palmitate plus ischemia-reperfusion. LP+DMD: low palmitate plus diamide. HP: high palmitate. HP+IR: high palmitate plus ischemia-reperfusion. HP+DMD: high palmitate plus diamide. *gpx3*: *glutathione peroxidase 3*. *grs*: *glutathione reductase*. *grx2*: *glutaredoxin 2*. *gss*: *glutathione synthetase*.

The mRNA expression of genes involved in mitochondrial fusion and energetics ('*hypoxia induced gene domain 1a*' (*higd1a*), '*hypoxia induced gene domain 2a*' (*higd2a*), '*mitofusin 1*' (*mfn1*), '*mitofusin 2*' (*mfn2*), and '*optic atrophy 1*' (*opa1*)) was also measured for this thesis (figure 22). We were not able to determine significant differences between any of the groups.

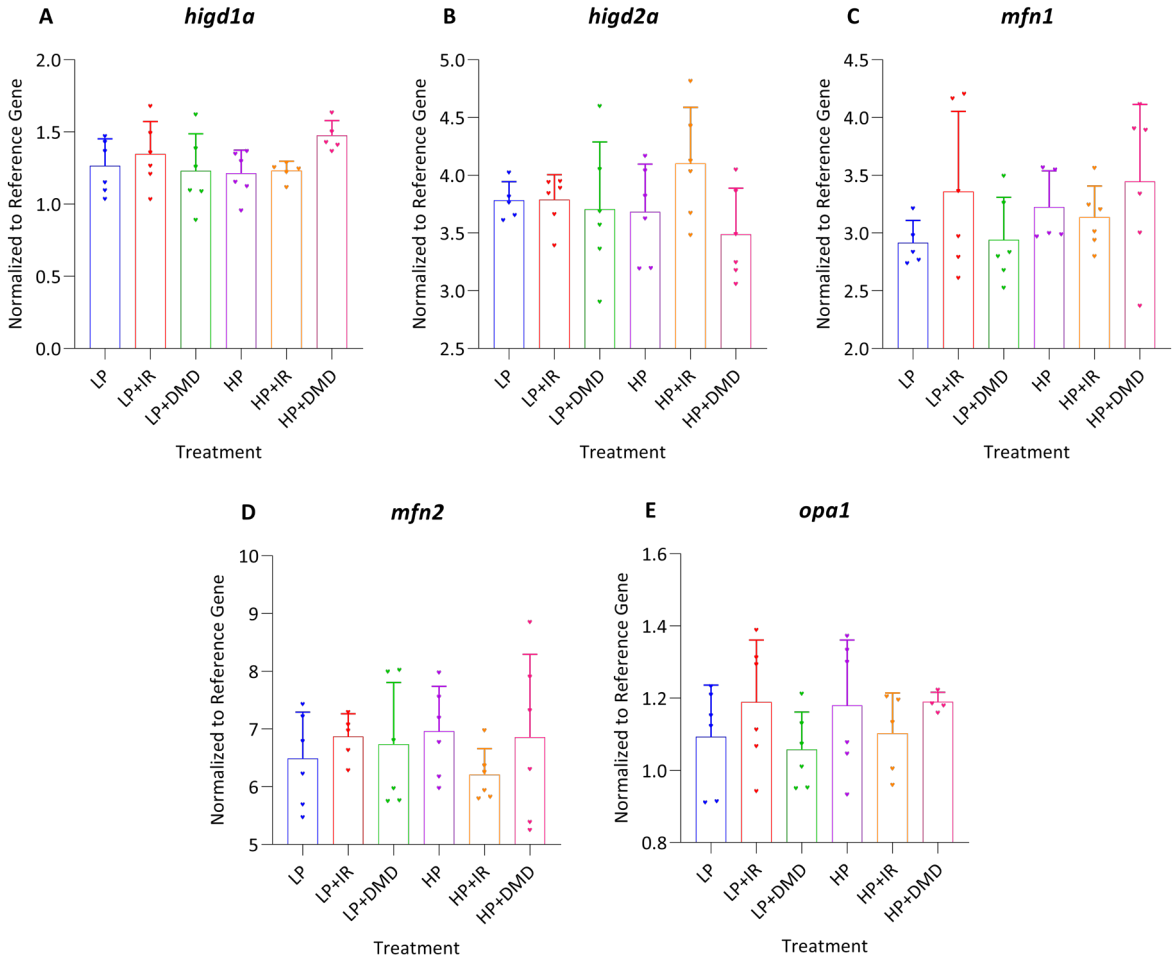

Figure 22. The analyzed genes related to mitochondrial function and dynamics. N=4-6. One-way ANOVA and Holm-Sidak multiple comparison tests were used for statistical analysis. Data are represented as means ± SD. IR: ischemia-reperfusion. LP: low palmitate. LP+IR: low palmitate plus ischemia-reperfusion. LP+DMD: low palmitate plus diamide. HP: high palmitate. HP+IR: high palmitate plus ischemia-reperfusion. HP+DMD: high palmitate plus

diamide. *higd1a*: *hypoxia induced gene domain 1a*. *higd2a*: *hypoxia induced gene domain 2a*. *mfn1*: *mitofusin 1*. *mfn2*: *mitofusin 2*. *opa1*: *optic atrophy 1*.

4.6 Protein S-Glutathionylation is neither Altered by Palmitate nor Diamide

There were no significance differences in levels of S-glutathionylated proteins in heart tissue observed between the groups (figure 23). A representative example of an S-glutathionylation blot (figure 24A) and the corresponding nitrocellulose membrane stained by ponceau (figure 24B) can be seen in figure 24. Samples that were treated with β-ME, which prevents glutathionylation, were also included as a negative control (appendix XVII).

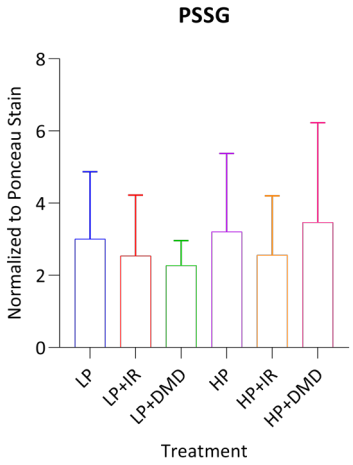

Figure 23. Global protein glutathionylation levels in homogenized tissue from hearts perfused with either low or high palmitate, following ischemia-reperfusion or diamide treatment. N=4-6. One-way ANOVA and Holm-Sidak multiple comparison tests were used for statistical analysis. Data are represented as means ± SD. IR: ischemia-reperfusion. LP: low palmitate. LP+IR: low palmitate plus ischemia-reperfusion. LP+DMD: low palmitate plus diamide. HP: high palmitate. HP+IR: high palmitate plus ischemia-reperfusion. HP+DMD: high palmitate plus diamide. PSSG: protein S-glutathionylation.

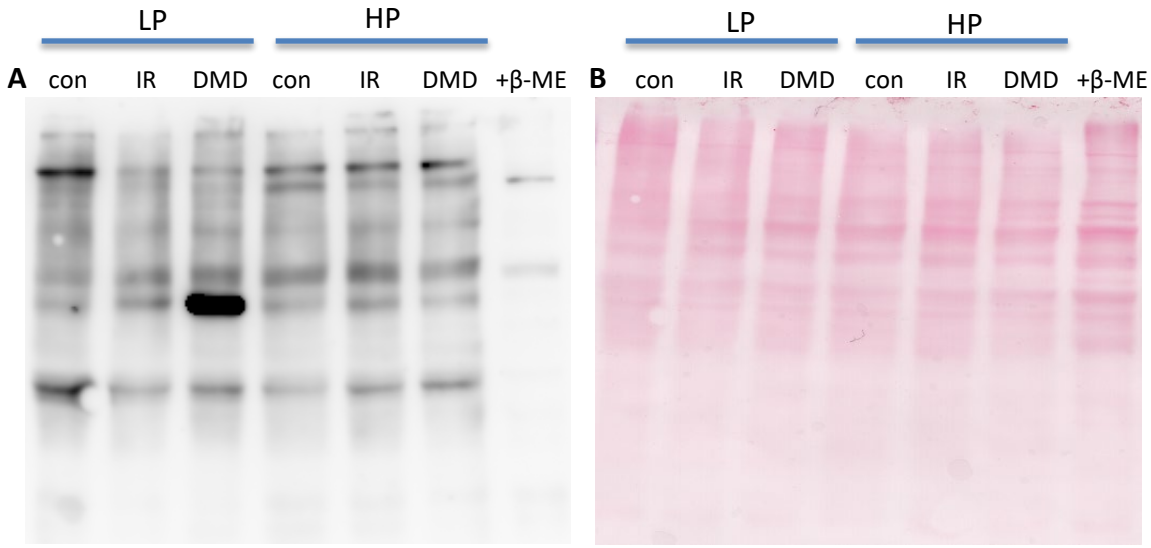

Figure 24. A representative example of an A) S-glutathionylation blot and B) ponceau stain of the same membrane, to assess total protein glutathionylation in the heart following IR or diamide treatment in hearts perfused with LP or HP. N=1. LP:low palmitate. HP:high palmitate. con: control. IR: ischemia-reperfusion. DMD: diamide. β-ME: β-mercaptoethanol.

5 Discussion

The heart preferentially uses fatty acids as a source of energy. In line with this, heart failure of different etiologies, including myocardial infarction, is associated with impaired fatty acid metabolism. Fatty acid oxidation increases NADPH regeneration in the TCA cycle, and NADPH is used by glutathione reductase (GRS) to convert GSSG back to GSH. As GSH is a major cellular antioxidant and has a central role in redox homeostasis [14], fatty acids therefore contribute to the maintenance of redox balance in the cells [15]. Changes in GSH/GSSG in the heart can induce arrhythmias, and increase susceptibility to IR injury [50]. In the present study, we wanted to examine whether the elevation of fatty acids contributed to changes in glutathione redox under conditions of cardiac stress.

Although no significant effect of palmitate could be observed in the present study in terms of cardiac function, HP perfusion in isolated hearts has been demonstrated to increase fatty acid oxidation and myocardial oxygen consumption while lowering cardiac efficiency [51] [52] [10] [53].

After a period of stabilization, the hearts that were exposed to IR treatment of this study underwent 17 minutes ischemia which was followed by 5 minutes reperfusion. Based on previous studies [54] [55], an ischemic period of 17 minutes was chosen, as this time induced cardiac stunning however did not damage the heart to such an extent that it would not recover function at all. The reperfusion period was determined to be 5 minutes as this was when we hypothesized that GSH/GSSG would be altered to the greatest extent [56].

Liu et al. have demonstrated that the presence of HP made the recovery after IR worse [57] but in the present study we did not find that HP worsened either cardiac output or cardiac power following IR. This may be due to the fact that both the ischemic and reperfusion periods were shorter than that used by Liu et al., 20 and 40 minutes, respectively. However, in agreement with the present study, the exposure to HP levels did not worsen infarct size or post-ischemic functional recovery despite an ischemia and a reperfusion that were slightly longer, 25 and 90 minutes, respectively) [10].

Early reperfusion is associated with a high release of ROS and altered redox environment as well as myocardial stunning. Therefore, this was a period where GSH/GSSG might be altered as shown in other studies that have demonstrated altered GSH/GSSG following IR [58] [59] [60]. In the present study, IR did not significantly affect either GSH or GSSG levels. A reason for this discrepancy may be the timepoints at which GSH/GSSG is measured. In the present study, the protocol included 17 minutes ischemia followed by 5 minutes of reperfusion, whereas GSH/GSSG was measured at 30 [58] [59] and 40 minutes [60] previously. It is possible that changes in GSH/GSSG could have been observed in the present study if we had also obtained measurements at a later timepoint in reperfusion.

However, protein S-glutathionylation has been reported to be increased at the start of reperfusion, 0-1 minute, and to decrease with time of reperfusion [56]. As we did not observe altered levels of protein S-glutathionylation between the experimental groups, it may be due to that this was measured at 5 minutes reperfusion in the present study. In summary, this timepoint may have been too short to observe significantly altered GSH/GSSG, but too long to observe changes in protein S-glutathionylation.

It has previously been shown that HP was associated with significantly decreased mitochondrial respiration in the CI OXPHOS state while does not alter the state of CI LEAK markedly [10]. In the present study, we have also found that HP does not affect the CI LEAK state of mitochondrial respiration but to some extent can depress the mitochondrial respiration in the CI OXPHOS state.

In the present study we did not find any significant effect of IR on the CI OXPHOS state of mitochondrial respiration in hearts perfused with either LP or HP. In contrast, Jespersen et al. reported IR treatment to lower CI OXPHOS [61]. Unlike the present study, the hearts of their experiments were perfused over a longer period of time and underwent a global no-flow ischemia for 30 minutes followed by 30 minutes of reperfusion.

It has been reported that increased utilization of fatty acids which is due to high dietary fat enhances mitochondrial H_2O_2 production and oxidative stress [62]. Jespersen et al. also show increased H_2O_2 emission during CI OXPHOS due to IR [61]. But in the present study, we did not observe any changes in H_2O_2 emission either with HP alone or following IR. In the latter study 30 minutes of reperfusion was followed by 30 minutes of a global no-flow ischemia while we used a global no-flow ischemia for 15 minutes following 5 minutes of a reperfusion period. This difference in the experimental designs could be the reason of insignificant differences in our data compared to theirs. Therefore, we may have seen a significant difference in H_2O_2 emission within the groups of our study if we had used a longer ischemic period.

We normalized the data of mitochondrial respiration and H_2O_2 emission to the activity of CS enzyme in the cardiac tissue homogenate. The reason why we used this normalization method is that CS is an enzymatic mitochondrial matrix marker [39] therefore its activity is a good indicator of how many mitochondria there are in the sample. It is important to consider that CS can be acutely altered by exercise [63] [64] and increased during postnatal development [65] however this was not relevant for the present study. This method of normalization has also been used by Lou et al. to normalize the measured oxygen consumption in perfused rat hearts [66]. Jespersen et al., however, have used the cardiac muscle mass to normalize the oxygen flux [61] and Boardman et al. have used protein content to normalize mitochondrial

respiration rates [10]. In summary, there is not one ideal marker to measure the amount of mitochondria present in the sample and precise determination can be difficult [39]. Therefore, it is of importance to consider whether the intervention being studied may alter either the mitochondrial quantity or quality, such that the mitochondrial marker itself is also altered by the intervention [39].

In another treatment of our study we used the pro-oxidant diamide to oxidize GSH as a positive control for GSH/GSSG analysis. Previous studies have shown that 200 µM diamide causes a dramatic increase in GSSG content while significantly decreases GSH and GSH/GSSG [50] and causes oxidative stess in the heart [67]. Fraiser et al. also show that GSH oxidation causes cardiac arrhythmias that may have contributed to decreased cardiac power and output in diamide-treated hearts in the present study [68]. The presence of HP did not alter cardiac output or cardiac power in the diamide-treated group, despite that GSSG was significantly lower. Future studies should include evaluation of cardiac arrhythmias under these conditions.

The most important proteins involved in mitochondrial fusion are 'optic atrophy 1' (OPA1), 'mitofusin 1' (MFN1) and 'mitofusin 2' (MFN2) and have been shown to play a role in remodelling of mitochondrial cristae [69]. Shutt et al. have observed that the monomeric and oligomeric forms of OPA1 are elevated when GSSG levels are high [70]. Therefore, we would have expected to see changes in these, especially in the hearts that were treated with diamide. However, we did not find these to be significantly altered in the present study.

We, nevertheless, found that the mRNA expression of '*glutathione reductase*' (*grs*), which reduces GSSG to GSH [31], and '*glutathione synthetase*' (*gss*), which synthesizes GSH in the cytoplasm [71], is alterted by low and high concentrations of palmitate respectively in the treatments containing diamide. Expression levels of '*glutathione reductase*' (*grs*) is elevated in LP perfused hearts treated with diamide but not when hearts are perfused with HP. In contrast, '*glutathione synthetase*' (*gss*) expression is elevated in HP perfused hearts treated with diamide but not when hearts are perfused with LP. So, the palmitate concentration stimulated different changes in glutathione synthesis. The LP stimulates the reduction of GSSG

back to GSH while the HP may be involved in increased GSH synthesis. Future experiments can be performed to examine this phenomenon in depth.

6 Conclusion

Although palmitate alone did not demonstrate any significant effect on the cardiac function, GSH content, GSH/GSSG, mitochondrial respiration, H_2O_2 emission, protein S-glutathionylation, and the expression of mitochondrial dynamics and glutathione-related genes, HP was associated with significantly decreased GSSG content following severe oxidative stress in the diamide-treated hearts. In addition, there was a difference in the expression of genes related to glutathione production in LP versus HP-perfused hearts. IR, however, was able to influence the cardiac function but did not have any huge impact on other parameters. The diamide pro-oxidant, in contrast, was extremely effective in altering most of the studied phenomena.

References

1. Stanley, W.C., F.A. Recchia, and G.D. Lopaschuk, *Myocardial Substrate Metabolism in the Normal and Failing Heart.* Physiological Reviews, 2005. **85**(3): p. 1093-1129.
2. McMurray, J.J.V. and M.A. Pfeffer, *Heart failure.* The Lancet, 2005. **365**(9474): p. 1877-1889.
3. Lopaschuk, G.D.*, et al.*, *Myocardial Fatty Acid Metabolism in Health and Disease.* Physiological Reviews, 2010. **90**(1): p. 207-258.
4. Ferrari, R., A. Cargnoni, and C. Ceconi, *Anti-ischaemic effect of ivabradine.* Pharmacological Research, 2006. **53**(5): p. 435-439.
5. Opie, L.H., *Chapter 2 - Cardiac Metabolism in Health and Disease*, in *Cellular and Molecular Pathobiology of Cardiovascular Disease*, M.S. Willis, J.W. Homeister, and J.R. Stone, Editors. 2014, Academic Press: San Diego. p. 23-36.
6. Lopaschuk, G.D.*, et al.*, *Plasma fatty acid levels in infants and adults after myocardial ischemia.* American Heart Journal, 1994. **128**(1): p. 61-67.
7. Opie, L.H., *Metabolism of free fatty acids, glucose and catecholamines in acute myocardial infarction: Relation to myocardial ischemia and infarct size.* The American Journal of Cardiology, 1975. **36**(7): p. 938-953.
8. Jaswal, J.S.*, et al.*, *Targeting fatty acid and carbohydrate oxidation — A novel therapeutic intervention in the ischemic and failing heart.* Biochimica et Biophysica Acta (BBA) - Molecular Cell Research, 2011. **1813**(7): p. 1333-1350.
9. Nagendran, J.*, et al.*, *Cardiomyocyte-specific ablation of CD36 improves post-ischemic functional recovery.* Journal of Molecular and Cellular Cardiology, 2013. **63**: p. 180-188.
10. Boardman, N.T.*, et al.*, *Diet-induced obese mouse hearts tolerate an acute high-fatty acid exposure that also increases ischemic tolerance.* American Journal of Physiology-Heart and Circulatory Physiology, 2020. **319**(3): p. H682-H693.
11. Veech, R.L., *Tricarboxylic Acid Cycle*, in *Encyclopedia of Biological Chemistry (Second Edition)*, W.J. Lennarz and M.D. Lane, Editors. 2013, Academic Press: Waltham. p. 436-440.

12. Mailloux, R.J., *Teaching the fundamentals of electron transfer reactions in mitochondria and the production and detection of reactive oxygen species.* Redox Biology, 2015. **4**: p. 381-398.
13. Opie, L.H., *Heart Physiology: From Cell to Circulation*. https://books.google.no/books?id=CPVSg69CPMsC2004: Lippincott Williams & Wilkins.
14. Dey, S., A. Sidor, and B. O'Rourke, *Compartment-specific Control of Reactive Oxygen Species Scavenging by Antioxidant Pathway Enzymes*.* Journal of Biological Chemistry, 2016. **291**(21): p. 11185-11197.
15. Kalucka, J.*, et al.*, *Quiescent Endothelial Cells Upregulate Fatty Acid β-Oxidation for Vasculoprotection via Redox Homeostasis.* Cell Metabolism, 2018. **28**(6): p. 881-894.e13.
16. Polyzos, A.A. and C.T. McMurray, *The chicken or the egg: mitochondrial dysfunction as a cause or consequence of toxicity in Huntington's disease.* Mechanisms of Ageing and Development, 2017. **161**: p. 181-197.
17. Cardol, P.*, et al.*, *Chapter 13 - Oxidative Phosphorylation: Building Blocks and Related Components*, in *The Chlamydomonas Sourcebook (Second Edition)*, E.H. Harris, D.B. Stern, and G.B. Witman, Editors. 2009, Academic Press: London. p. 469-502.
18. Sousa, J.S., E. D'Imprima, and J. Vonck, *Mitochondrial Respiratory Chain Complexes*, in *Membrane Protein Complexes: Structure and Function*, J.R. Harris and E.J. Boekema, Editors. 2018, Springer Singapore: Singapore. p. 167-227.
19. Ricquier, D. and F. Bouillaud, *Uncoupling Proteins*, in *Encyclopedia of Biological Chemistry (Second Edition)*, W.J. Lennarz and M.D. Lane, Editors. 2013, Academic Press: Waltham. p. 482-487.
20. Rousset, S.*, et al.*, *The Biology of Mitochondrial Uncoupling Proteins.* Diabetes, 2004. **53**(suppl 1): p. S130-S135.
21. Rolfe, D.F.S. and M.D. Brand, *The Physiological Significance of Mitochondrial Proton Leak in Animal Cells and Tissues.* Bioscience Reports, 1997. **17**(1): p. 9-16.

22. Ray, P.D., B.-W. Huang, and Y. Tsuji, *Reactive oxygen species (ROS) homeostasis and redox regulation in cellular signaling.* Cellular signalling, 2012. **24**(5): p. 981-990.
23. Brand, M.D., *The sites and topology of mitochondrial superoxide production.* Experimental gerontology, 2010. **45**(7-8): p. 466-472.
24. Desa, D.E., M.G. Nichols, and H.J. Smith, *Aminoglycosides rapidly inhibit NAD(P)H metabolism increasing reactive oxygen species and cochlear cell demise.* Journal of biomedical optics, 2018. **24**(5): p. 1-14.
25. Hausenloy, D.J. and D.M. Yellon, *Myocardial ischemia-reperfusion injury: a neglected therapeutic target.* The Journal of Clinical Investigation, 2013. **123**(1): p. 92-100.
26. Fisher-Wellman, K.H.*, et al.*, *Pyruvate dehydrogenase complex and nicotinamide nucleotide transhydrogenase constitute an energy-consuming redox circuit.* The Biochemical journal, 2015. **467**(2): p. 271-280.
27. Pompella, A.*, et al.*, *The changing faces of glutathione, a cellular protagonist.* Biochemical Pharmacology, 2003. **66**(8): p. 1499-1503.
28. Aon, M.A.*, et al.*, *Sequential Opening of Mitochondrial Ion Channels as a Function of Glutathione Redox Thiol Status*.* Journal of Biological Chemistry, 2007. **282**(30): p. 21889-21900.
29. Ulrich, K. and U. Jakob, *The role of thiols in antioxidant systems.* Free Radical Biology and Medicine, 2019. **140**: p. 14-27.
30. Aon, M.A., S. Cortassa, and B. O'Rourke, *Redox-optimized ROS balance: a unifying hypothesis.* Biochimica et biophysica acta, 2010. **1797**(6-7): p. 865-877.
31. Murphy, M.P., *Mitochondrial Thiols in Antioxidant Protection and Redox Signaling: Distinct Roles for Glutathionylation and Other Thiol Modifications.* Antioxidants & Redox Signaling, 2011. **16**(6): p. 476-495.
32. Xiong, Y.*, et al.*, *S-glutathionylation: from molecular mechanisms to health outcomes.* Antioxidants & redox signaling, 2011. **15**(1): p. 233-270.
33. Westermann, B., *Mitochondrial fusion and fission in cell life and death.* Nature Reviews Molecular Cell Biology, 2010. **11**(12): p. 872-884.

34. Issop, L., M.B. Rone, and V. Papadopoulos, *Organelle plasticity and interactions in cholesterol transport and steroid biosynthesis.* Molecular and Cellular Endocrinology, 2013. **371**(1): p. 34-46.

35. Liu, Y.J.*, et al.*, *Mitochondrial fission and fusion: A dynamic role in aging and potential target for age-related disease.* Mechanisms of Ageing and Development, 2020. **186**: p. 111212.

36. van der Vusse, G.J., *Albumin as Fatty Acid Transporter.* Drug Metabolism and Pharmacokinetics, 2009. **24**(4): p. 300-307.

37. McNeill, J.H., *Measurement of Cardiac Function*. https://books.google.no/books?id=RRv7wAEACAAJ1996: CRC-Press.

38. Baker, M.A. and B.A. Hagner, *Diamide induced shift in protein and glutathione thiol: disulfide status delays DNA rejoining after X-irradiation of human cancer cells.* Biochimica et Biophysica Acta (BBA) - Protein Structure and Molecular Enzymology, 1990. **1037**(1): p. 39-47.

39. Gnaiger Erich*, et al.*, *Mitochondrial respiratory states and rates.* Bioenergetics Communications, 2019. 10.26124/mitofit:190001.v6.

40. Makrecka-Kuka, M., G. Krumschnabel, and E. Gnaiger, *High-Resolution Respirometry for Simultaneous Measurement of Oxygen and Hydrogen Peroxide Fluxes in Permeabilized Cells, Tissue Homogenate and Isolated Mitochondria.* Biomolecules, 2015. **5**(3): p. 1319-1338.

41. Krumschnabel, G.*, et al.*, *Simultaneous High-Resolution Measurement of Mitochondrial Respiration and Hydrogen Peroxide Production*, in *Mitochondrial Medicine: Volume I, Probing Mitochondrial Function*, V. Weissig and M. Edeas, Editors. 2015, Springer New York: New York, NY. p. 245-261.

42. Murphy, M.P., *How mitochondria produce reactive oxygen species.* The Biochemical journal, 2009. **417**(1): p. 1-13.

43. Perry, J.B.*, et al.*, *Cardioprotective effects of idebenone do not involve ROS scavenging: Evidence for mitochondrial complex I bypass in ischemia/reperfusion injury.* Journal of Molecular and Cellular Cardiology, 2019. **135**: p. 160-171.

44. Hoffman, D.L. and P.S. Brookes, *Oxygen Sensitivity of Mitochondrial Reactive Oxygen Species Generation Depends on Metabolic Conditions.* Journal of Biological Chemistry, 2009. **284**(24): p. 16236-16245.

45. Vandesompele, J.*, et al.*, *Accurate normalization of real-time quantitative RT-PCR data by geometric averaging of multiple internal control genes.* Genome Biology, 2002. **3**(7): p. research0034.1.

46. Florholmen-Kjær, Å.*, et al.*, *A sensitive method for the analysis of glutathione in porcine hepatocytes.* Scandinavian Journal of Gastroenterology, 2014. **49**(11): p. 1359-1366.

47. Aebersold, R. and M. Mann, *Mass-spectrometric exploration of proteome structure and function.* Nature, 2016. **537**(7620): p. 347-355.

48. Schindelin, J.*, et al.*, *Fiji: an open-source platform for biological-image analysis.* Nature Methods, 2012. **9**(7): p. 676-682.

49. Gnaiger, E.*, et al.*, *Mitochondrial coupling and capacity of oxidative phosphorylation in skeletal muscle of Inuit and Caucasians in the arctic winter.* Scandinavian Journal of Medicine & Science in Sports, 2015. **25**(S4): p. 126-134.

50. Brown, D.A.*, et al.*, *Cardiac arrhythmias induced by glutathione oxidation can be inhibited by preventing mitochondrial depolarization.* Journal of molecular and cellular cardiology, 2010. **48**(4): p. 673-679.

51. Mazumder, P.K.*, et al.*, *Impaired Cardiac Efficiency and Increased Fatty Acid Oxidation in Insulin-Resistant ob/ob Mouse Hearts.* Diabetes, 2004. **53**(9): p. 2366.

52. Cole, M.A.*, et al.*, *A high fat diet increases mitochondrial fatty acid oxidation and uncoupling to decrease efficiency in rat heart.* Basic research in cardiology, 2011. **106**(3): p. 447-457.

53. How, O.-J.*, et al.*, *Increased Myocardial Oxygen Consumption Reduces Cardiac Efficiency in Diabetic Mice.* Diabetes, 2006. **55**(2): p. 466.

54. Aasum, E., A.D. Hafstad, and T.S. Larsen, *Change in substrate metabolism in isolated mouse hearts following ischemia-reperfusion.* Molecular and Cellular Biochemistry, 2003. **249**(1): p. 97-103.

55. De Windt, L.J.*, et al.*, *Ischemic-reperfused isolated working mouse hearts: membrane damage and type IIA phospholipase A2.* American Journal of Physiology-Heart and Circulatory Physiology, 2001. **280**(6): p. H2572-H2580.

56. Eaton, P.*, et al.*, *Glyceraldehyde Phosphate Dehydrogenase Oxidation During Cardiac Ischemia and Reperfusion.* Journal of Molecular and Cellular Cardiology, 2002. **34**(11): p. 1549-1560.

57. Liu, Q.*, et al.*, *High levels of fatty acids delay the recoveryof intracellular pH and cardiac efficiency inpost-ischemic hearts by inhibiting glucose oxidation.* Journal of the American College of Cardiology, 2002. **39**(4): p. 718-725.

58. Marina Prendes, M.G.*, et al.*, *Involvement of energetic metabolism in the effects of ischemic postconditioning on the ischemic-reperfused heart of fed and fasted rats.* The Journal of Physiological Sciences, 2011. **61**(4): p. 303-312.

59. Marina Prendes, M.G.*, et al.*, *INVOLVEMENT OF MITOCHONDRIAL PERMEABILITY TRANSITION, GLUTATHIONE STATUS, PENTOSE PHOSPHATE PATHWAY AND OXIDATIVE DAMAGE IN THE PROTECTIVE EFFECT OF FASTING ON THE ISCHAEMIC-REPERFUSED RAT HEART.* Clinical and Experimental Pharmacology and Physiology, 2009. **36**(7): p. 637-642.

60. Haramaki, N.*, et al.*, *Networking Antioxidants in the Isolated Rat Heart are Selectively Depleted by Ischemia-Reperfusion.* Free Radical Biology and Medicine, 1998. **25**(3): p. 329-339.

61. Jespersen, N.R.*, et al.*, *Pre-ischaemic mitochondrial substrate constraint by inhibition of malate-aspartate shuttle preserves mitochondrial function after ischaemia-reperfusion.* The Journal of physiology, 2017. **595**(12): p. 3765-3780.

62. Rindler, P.M.*, et al.*, *Redox regulation of insulin sensitivity due to enhanced fatty acid utilization in the mitochondria.* American Journal of Physiology-Heart and Circulatory Physiology, 2013. **305**(5): p. H634-H643.

63. Tonkonogi, M., B. Harris, and K. Sahlin, *Increased activity of citrate synthase in human skeletal muscle after a single bout of prolonged exercise.* Acta Physiologica Scandinavica, 1997. **161**(3): p. 435-436.

64. Leek, B.T.*, et al.*, *Effect of acute exercise on citrate synthase activity in untrained and trained human skeletal muscle.* American Journal of Physiology-Regulatory, Integrative and Comparative Physiology, 2001. **280**(2): p. R441-R447.

65. Drahota, Z.*, et al.*, *Developmental changes of cytochrome c oxidase and citrate synthase in rat heart homogenate.* Physiol Res, 2004. **53**(1): p. 119-22.

66. Lou, P.-H.*, et al.*, *The mechanism of Intralipid®-mediated cardioprotection complex IV inhibition by the active metabolite, palmitoylcarnitine, generates reactive oxygen species and activates reperfusion injury salvage kinases.* PloS one, 2014. **9**(1): p. e87205-e87205.

67. Xie, C.*, et al.*, *Glutathione oxidation unmasks proarrhythmic vulnerability of chronically hyperglycemic guinea pigs.* American journal of physiology. Heart and circulatory physiology, 2013. **304**(7): p. H916-H926.

68. Frasier, C.R.*, et al.*, *Short-term exercise preserves myocardial glutathione and decreases arrhythmias after thiol oxidation and ischemia in isolated rat hearts.* Journal of Applied Physiology, 2011. **111**(6): p. 1751-1759.

69. Hernandez-Resendiz, S.*, et al.*, *Targeting mitochondrial fusion and fission proteins for cardioprotection.* Journal of Cellular and Molecular Medicine, 2020. **24**(12): p. 6571-6585.

70. Shutt, T.*, et al.*, *The intracellular redox state is a core determinant of mitochondrial fusion.* EMBO reports, 2012. **13**(10): p. 909-915.

71. Marí, M.*, et al.*, *Mitochondrial Glutathione, a Key Survival Antioxidant.* Antioxidants & Redox Signaling, 2009. **11**(11): p. 2685-2700.

Appendices

Appendix I

Table A I. The salty components of Krebs-Henseleit buffer (KHB).

Salt	Molecular weight	Final concentration (M)
Sodium chloride (NaCl)	58.44	118.5
Potassium chloride (KCl)	74.55	4.7
Monopotassium phosphate (KH_2PO_4)	136.09	1.2
Magnesium sulfate ($MgSO_4.7H_2O$)	246.48	1.2
Calcium chloride ($CaCl_2.2H_2O$)	147.02	2.25

Appendix II

Table A II. The components of A1 solution (pH=7.4 at 0°C).

Chemical	Molecular weight	Final concentration (mM)
Sucrose ($C_{12}H_{22}O_{11}$)	342.3	250
EDTA (Ethylenediaminetetraacetic acid) di sodium ($Na_2C_{10}H_{16}N_2O_8$)	372.2	0.5
Tris ($C_4H_{11}NO_3$)	121.1	10

Appendix III

Table A III. The components of mitochondrial respiration medium 05 (MiR05) (pH=7.1 at 30°C).

Chemical	Molecular weight	Final concentration
EGTA (Triethylene glycol diamine tetraacetic acid) $C_{14}H_{24}N_2O_{10}$	380.4	0.5 mM
Magnesium chloride ($MgCl_2.6H_2O$)	203.3	3 mM
Taurine ($C_2H_7NO_3S$)	125.1	20 mM
Monopotassium phosphate (KH_2PO_4)	136.1	10 mM
HEPES ($C_8H_{18}N_2O_4S$)	238.3	20 mM
Sucrose ($C_{12}H_{22}O_{11)}$	342.3	110 mM
Potassium lactobionate ($C_{12}H_{21}KO_{12}$) [0.5 M] (pH=7.0)	358.3	60 mM
Bovine Serum Albumin (BSA)	66.5 kDa	1 gr/L

Appendix IV

Table A IV. The sequences of the primers which were used in qPCR experiments for mRNA analysis. FP: forward primer. RP: reverse primer.

Gene	Primer sequence (5'-3')
Glutaredoxin 2 (grx2)	FP: ATCGTCGTTTTGGGGGAAGTC RP: GGAACAGTAAGAGCAGGATGTTT
Glutathione reductase (grs)	FP: ACTATGACAACATCCCTACTGTGG RP: CCCATACTTATGAACAGCTTCGT
glutathione peroxidase 3 (gpx3)	FP: AGAAGAGCGACGACAAACCC RP: AAAACCTGCTTCAACACTCGG
Glutathione synthetase (gss)	FP: AAAGCAGGCCATAGACAGGG RP: TGAATGGGGCATACGTCACC
Hypoxia induced gene domain 1a (higd1a)	FP: CTTGATCCACATGCGTGTAGC RP: TGATACATGGAGTAGCCCATACC
Hypoxia induced gene domain 1a (higd2a)	FP: AAGCCCCCAGTTATCGAGG RP: GGTGGAAGCAGTAAAGGCCA
Mitofusin 1 (mfn1)	FP: ATGGCAGAAACGGTATCTCCA RP: GCCCTCAGTAACAAACTCCAGT
Mitofusin 2 (mfn2)	FP: AGAACTGGACCCGGTTACCA RP: CACTTCGCTGATACCCCTGA

Optic atrophy 1 (opa1)	FP: TGGAAAATGGTTCGAGAGTCAG RP: CATTCCGTCTCTAGGTTAAAGCG

Appendix V

Table A V. The chemicals which were used in GSH/GSSG analysis. GSH: reduced glutathione, GSSG: glutathione disulfide.

Chemical	Component
Washing buffer (pH=7.4)	Phosphate ($[PO_4]^{3-}$) [10 mM] Sodium (Na^+) [17 mM] Sodium chloride (NaCl) [122 mM] Potassium chloride (KCl) [3 mM] Glucose ($C_6H_{12}O_6$) [5 mM]
Labeled GSH	GSH [32.22 mM] Acetic acid (CH_3COOH) [1 mM]
Labeled GSSG	Glutathione disulfide (GSSG) (Unknown concentration)
TCA (Trichloroacetic acid) (CCl_3COOH) [8 M]	
Dichloromethane (CH_2Cl_2) (Molecular Weight=84.93 gr/mol)	
N-ethylmaleimide (NEM) (pH=4)	N-ethylmaleimid (NEM) [60 mM] Dimethyl sulfoxide (DMSO) [128 mM] Acetic acid (CH_3COOH) [1 mM] Sodium chloride (NaCl) [150 mM]

GSH (pH=4)	GSH [102.4 mM] Acetic acid (CH3COOH) [10 mM]
GSSG (pH=4)	GSSG [12.8 mM] Sodium (Na^+) [25.6 mM]

Appendix VI

Table A VI. The standards which were used in GSH/GSSG analysis. GSH: reduced glutathione, GSSG: glutathione disulfide.

Standard	Component
Internal standard 1 (GSH) (pH=4)	GSH [0.06 mM] Acetic acid (CH_3COOH) [1 mM] Sodium chloride (NaCl) [150 mM]
Internal standard 2 (GSSG) (pH=4)	GSSG Acetic acid (CH_3COOH) [1 mM] Sodium chloride (NaCl) [150 mM]
GSH 1	GSH [256 µM]
GSH 2	GSH [128 µM]
GSH 3	GSH [64 µM]
GSH 4	GSH [32 µM]
GSH 5	GSH [16 µM]
GSH 6	GSH [8 µM]
GSSG 1	GSSG [15 µM]
GSSG 2	GSSG [12 µM]
GSSG 3	GSSG [10 µM]
GSSG 4	GSSG [6 µM]

GSSG 5	GSSG [4 µM]
GSSG 6	GSSG [2 µM]
GSSG 7	GSSG [0.04 µM]
GSSG 8	GSSG [0.02 µM]
GSSG 9	GSSG [0.004 µM]
GSSG 10	GSSG [0.002 µM]
GSSG 11	GSSG [0.0004 µM]
GSSG 12	GSSG [0.0002 µM]
GSSG 13	GSSG [0.00004 µM]
GSSG 14	GSSG [0 µM]

Appendix VII

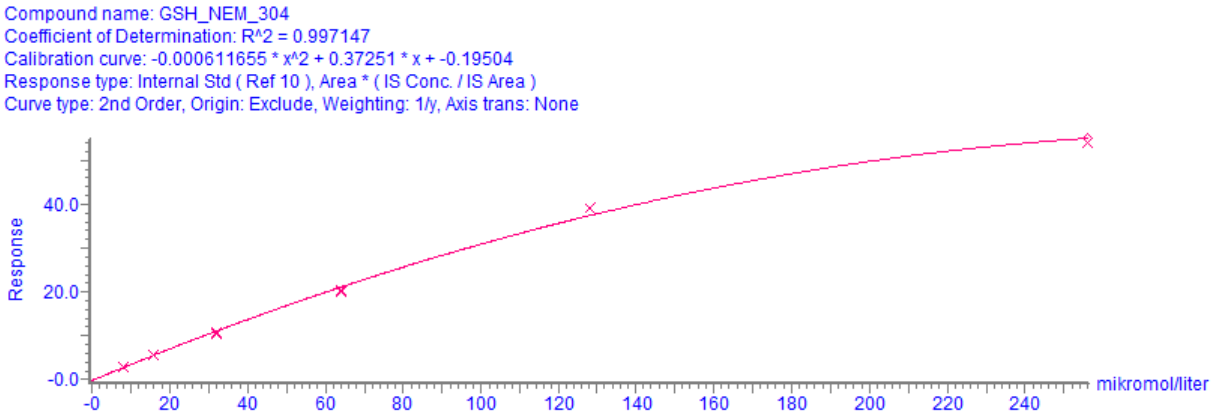

Figure A I. The standard curve of reduced glutathione (GSH) analyzed by LC-MS/MS (Liquid Chromatography Mass Spectrometry).

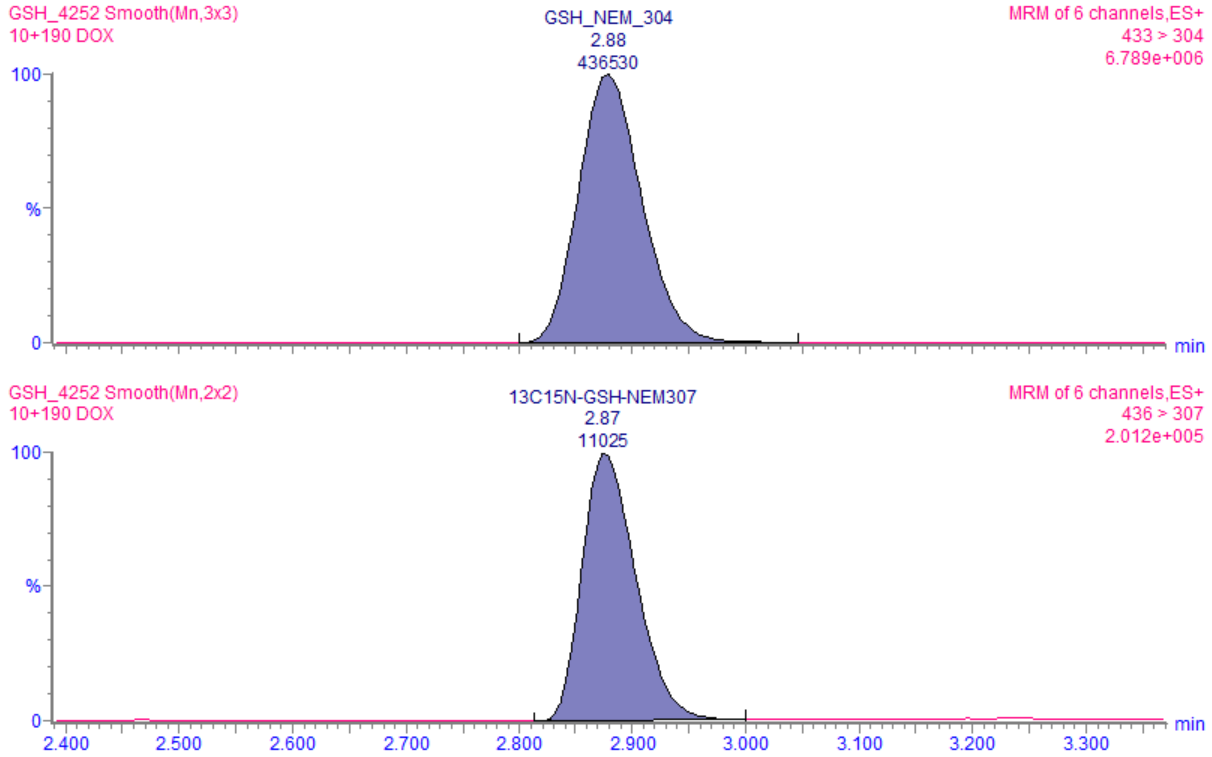

Figure A II. The peaks of reduced glutathione (GSH) analyzed by LC-MS/MS (Liquid Chromatography Mass Spectrometry).

Appendix VIII

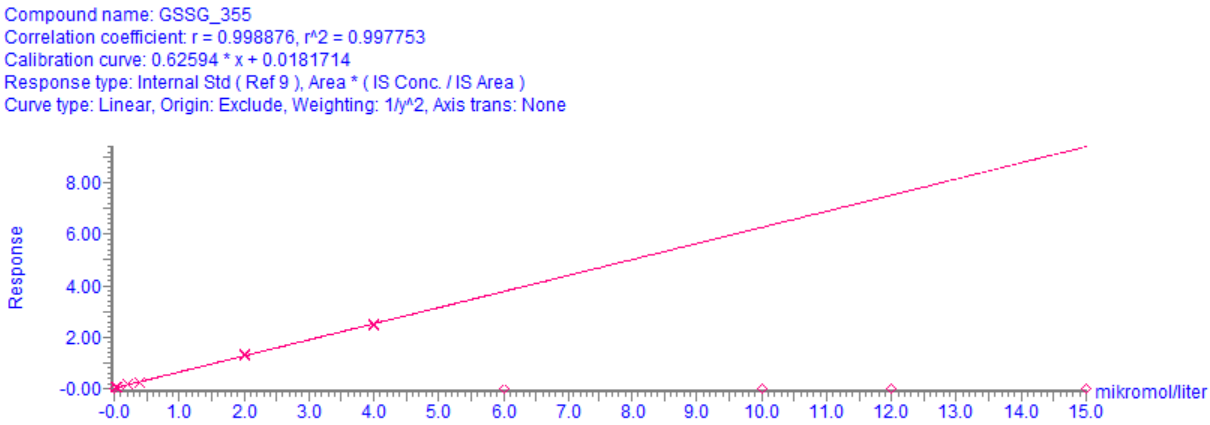

Figure A III. The standard curve of glutathione disulfide (GSSG) analyzed by LC-MS/MS (Liquid Chromatography Mass Spectrometry).

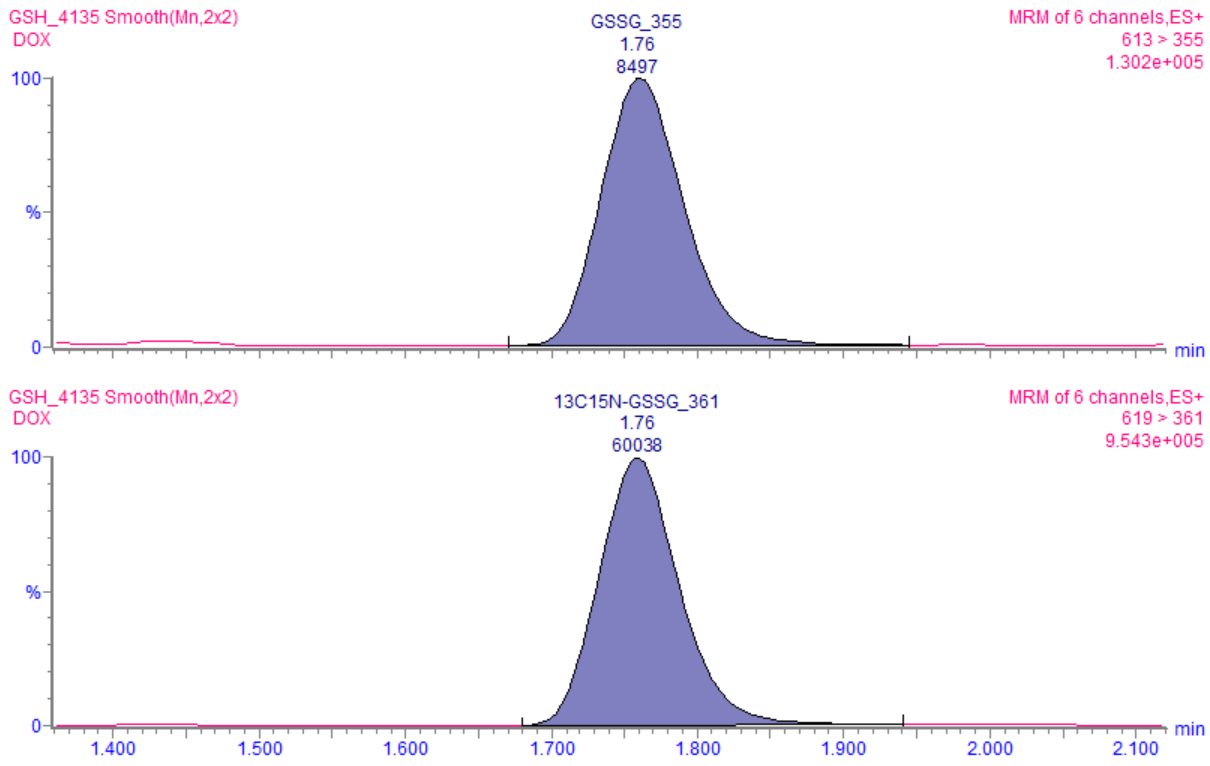

Figure A IV. The peaks of glutathione disulfide (GSSG) analyzed by LC-MS/MS (Liquid Chromatography Mass Spectrometry).

Appendix IX

Table A VII. The reagents which were used in serum non-esterified fatty acids (NEFA) quantitative determination.

Reagent	Component
R1 set	R1a (color A): ACS (Acyl-CoA synthetase) [0.53 U/mL] CoA (Coenzyme A) [0.31 mmol/L] ATP (Adenosine 5-triphosphate disodium salt) [4.3 mmol/L] 4-AA (4-amino-antipyrine) [1.5 mmol/L] AOD [2.6 U/mL] Sodium azide (0.062%) (Color A lyophilized) (0.8%) R1 (solvent A): Phosphate buffer (pH=7.0) [50 mmol/L] Sodium azide (0.05%)
R2 set	R2a (color B): ACOD (Acyl-CoA oxidase) [12 U/mL] POD (Peroxidase) [14 U/mL]

	R2 (solvent B): MEHA (3-Methyl-N-Ethyl-N-(β-Hydroxyethyl)-Aniline) [2.4 mmol/L]

Appendix X

Table A VIII. The components of the homogenization buffer (radioimmunoprecipitation assay (RIPA) buffer) for preparing western blotting samples.

Chemical	Final concentration
Tris-hydrocholoric acid ($C_4H_{11}NO_3$.HCl) (pH=8.0)	10 mM
EDTA (Ethylenediaminetetraacetic acid) di sodium ($Na_2C_{10}H_{16}N_2O_8$)	1 mM
EGTA (Triethylene glycol diamine tetraacetic acid) $C_{14}H_{24}N_2O_{10}$	0.5 mM
Triton X-100 ($C_{14}H_{22}O(C_2H_4O)_n$(n=9-10))	1%
Sodium deoxycholate ($C_{24}H_{39}NaO_4$)	0.1%
Sodium dodecyl sulfate (SDS) ($NaC_{12}H_{25}SO_4$)	0.1%
Sodium chloride (NaCl)	140 mM
Phenylmethylsulfonyl fluoride (PMSF) ($C_7H_7FO_2S$)	1 mM

Appendix XI

Table A IX. The components of 8% acrylamide resolving gel.

Chemical	Final concentration (%)
Acrylamide mix [30%]	8
Tris-hydrocholoric acid ($C_4H_{11}NO_3$.HCl) (pH=8.8) [1.5 M]	25
Sodium dodecyl sulfate (SDS) ($NaC_{12}H_{25}SO_4$) [10%]	0.1
Ammonium persulfate ($(NH_4)_2S_2O_8$) [10%]	0.1
Tetramethylethylenediamine (TEMED) ($C_6H_{16}N_2$) (non-diluted)	0.06

Appendix XII

Table A X. The components of 5% acrylamide stacking gel.

Chemical	Final concentration (%)
Acrylamide mix [30%]	5
Tris-hydrocholoric acid ($C_4H_{11}NO_3$.HCl) (pH=6.8) [0.5 M]	25
Sodium dodecyl sulfate (SDS) ($NaC_{12}H_{25}SO_4$) [10%]	0.1
Ammonium persulfate ($(NH_4)_2S_2O_8$) [10%]	0.1
Tetramethylethylenediamine (TEMED) ($C_6H_{16}N_{2)}$ (non-diluted)	0.1

Appendix XIII

Table A XI. The components of the electrophoresis running buffer (pH=8.8).

Chemical	Final concentration (gr/L)
Tris-basic ($C_4H_{11}NO_3$) [0.12 M]	3.02
Glycine ($C_2H_5NO_2$)	14.4
Sodium dodecyl sulfate (SDS) ($NaC_{12}H_{25}SO_4$)	1

Appendix XIV

Table A XII. The components of the electrophoresis transfer buffer (pH=8.3).

Chemical	Final concentration
Tris-basic ($C_4H_{11}NO_3$) [0.12 M]	3 gr/L
Glycine ($C_2H_5NO_2$)	14.4 gr/L
Methanol (CH_3OH)	20%

Appendix XV

Table A XIII. The components of the ponceau stain.

Chemical	Final concentration
Ponceau S ($C_{22}H_{12}N_4Na_4O_{13}S_4$)	5 gr/L
Acetic acid (CH_3COOH)	1%

Appendix XVI

Table A XIV. The components of the washing buffer (tris buffered saline-Tween 20 (TBS-T)) (pH=7.6).

Chemical	Final concentration
Tris-basic ($C_4H_{11}NO_3$)	2.42 gr/L
Sodium Chloride (NaCl)	8 gr/L
Polysorbate 20 (Tween 20) ($C_{58}H_{114}O_{26}$)	0.1%

Appendix XVII

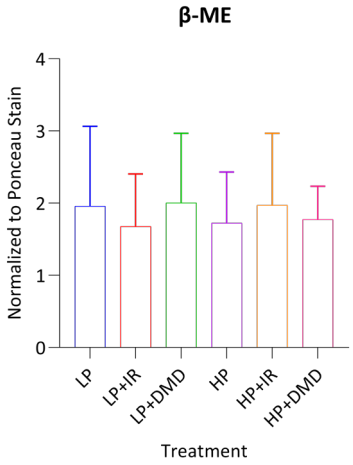

Figure A V. The samples which were treated with β-ME to serve as negative control for protein S-glutathionylation. N=2. One-way ANOVA and Holm-Sidak multiple comparison tests were used for statistical analysis. Data are represented as means ± SD. IR: ischemia-reperfusion. LP: low palmitate. LP+IR: low palmitate plus ischemia-reperfusion. LP+DMD: low palmitate plus diamide. HP: high palmitate. HP+IR: high palmitate plus ischemia-reperfusion. HP+DMD: high palmitate plus diamide. β-ME: β-mercaptoethanol.